


Article

Design, Synthesis and Biological Evaluation of Novel and Potent Protein Arginine Methyltransferases 5 Inhibitors for Cancer Therapy

Yixuan Tang ^{1,†} , Shihui Huang ^{1,†}, Xingxing Chen ¹, Junzhang Huang ¹, Qianwen Lin ¹, Lei Huang ¹, Shuping Wang ¹, Qihua Zhu ^{1,2}, Yungen Xu ^{1,2,*} and Yi Zou ^{1,*}

¹ Department of Medicinal Chemistry, School of Pharmacy, China Pharmaceutical University, Nanjing 210009, China

² Jiangsu Key Laboratory of Drug Design and Optimization, School of Pharmacy, China Pharmaceutical University, Nanjing 210009, China

* Correspondence: xyg@cpu.edu.cn (Y.X.); zyc138@163.com (Y.Z.); Tel.: +86-025-86185303 (Y.X.)

† These authors have contributed equally to this work.

Abstract: Protein arginine methyltransferases 5 (PRMT5) is a clinically promising epigenetic target that is upregulated in a variety of tumors. Currently, there are several PRMT5 inhibitors under preclinical or clinical development, however the established clinical inhibitors show favorable toxicity. Thus, it remains an unmet need to discover novel and structurally diverse PRMT5 inhibitors with characterized therapeutic utility. Herein, a series of tetrahydroisoquinoline (THIQ) derivatives were designed and synthesized as PRMT5 inhibitors using GSK-3326595 as the lead compound. Among them, compound 20 (IC₅₀: 4.2 nM) exhibits more potent PRMT5 inhibitory activity than GSK-3326595 (IC₅₀: 9.2 nM). In addition, compound 20 shows high anti-proliferative effects on MV-4-11 and MDA-MB-468 tumor cells and low cytotoxicity on AML-12 hepatocytes. Furthermore, compound 20 possesses acceptable pharmacokinetic profiles and displays considerable in vivo antitumor efficacy in a MV-4-11 xenograft model. Taken together, compound 20 is an antitumor compound worthy of further study.

Keywords: epigenetic; PRMT5 inhibitors; THIQ; cancer



Citation: Tang, Y.; Huang, S.; Chen, X.; Huang, J.; Lin, Q.; Huang, L.; Wang, S.; Zhu, Q.; Xu, Y.; Zou, Y. Design, Synthesis and Biological Evaluation of Novel and Potent Protein Arginine Methyltransferases 5 Inhibitors for Cancer Therapy. *Molecules* **2022**, *27*, 6637. <https://doi.org/10.3390/molecules27196637>

Academic Editor: Keykavous Parang

Received: 18 September 2022

Accepted: 3 October 2022

Published: 6 October 2022

Publisher's Note: MDPI stays neutral with regard to jurisdictional claims in published maps and institutional affiliations.



Copyright: © 2022 by the authors. Licensee MDPI, Basel, Switzerland. This article is an open access article distributed under the terms and conditions of the Creative Commons Attribution (CC BY) license (<https://creativecommons.org/licenses/by/4.0/>).

1. Introduction

Methylated arginine is a post-translational modification of proteins that exists in many cellular processes including transcription, DNA damage response, stem cell function, epigenetically mediated gene expression and immune response [1,2]. Arginine methylation is regulated by protein arginine methyltransferases (PRMTs). PRMTs transfer methyl group from S-adenosyl-L-methionine (SAM) to the substrate arginine side chain. PRMTs can be categorized into three subtypes: Type I PRMTs (PRMT1, PRMT2, PRMT3, CARM1/PRMT4, PRMT6, and PRMT8) catalyze formation of ω-NG-monomethyl-arginine (MMA) and ω-NG, NG-asymmetric dimethyl-arginine (aDMA), Type II PRMTs (PRMT5 and PRMT9) catalyze formation of MMA and ω-NG, N'G-symmetric dimethyl arginine (sDMA), whereas type III PRMT (PRMT7) catalyzes only formation of MMA [3–5].

PRMT5 belongs to the predominant type II PRMTs, which is found in nearly all eukaryotic species [6]. The N-terminal domain of PRMT5 adopts a triosephosphate isomerase barrel structure, which forms a stable complex with methylosome protein 50 (MEP50). MEP50, as the most important interacting partner of PRMT5, is essential for the catalytic activity of PRMT5 [7]. A variety of intracellular substances was methylated by PRMT5, including histone H4 residue Arg3 (H4R3) and H3 residue Arg8(H3R8), which mediated various cellular processes such as transcriptional repression [8,9]. PRMT5 overexpression is involved in the proliferation and survival of numerous different cancers, including

colorectal, lung, ovarian, prostate, and pancreatic cancers, and lymphoma, leukemia, and glioblastoma [10–15]. Interestingly, it is reported that shPRMT5 or PRMT5 inhibitors motivated cGas/ STING and NLRC5 pathway and repressed MYC downstream genes, which provided possibility to the combination therapy of PD-1 and PRMT5 inhibitors [16–18]. Consequently, targeting PRMT5 is being pursued as a new cancer therapeutic strategy.

In the past few years, tremendous efforts from academia and pharmaceutical companies have been made to discover and develop PRMT5 inhibitors, and several PRMT5 inhibitors are currently in clinical trials (Figure 1). As the active site of the enzyme consists of an SAM-binding pocket and a substrate-binding pocket, the mechanism of action of the clinical PRMT5 inhibitors can be classified into SAM-uncompetitive (GSK-3326595 [19], EPZ015666 [20]) and SAM-competitive (JNJ64619178 [21], PF06939999 [22]) inhibitors. In addition, there are some reports about PRMT5 allosteric inhibition, covalent inhibition and PROTACS [23–25]. GSK-3326595 from GlaxoSmithKline is an SAM-uncompetitive PRMT5 inhibitor, which has good brain permeability and anti-tumor effect, and is currently in clinical phase I/II (NCT04676516). Due to the lack of selectivity for tumor cells and normal cells, however, GSK-3326595 caused grade 3 or 4 adverse events in clinical studies. Therefore, the search for safe and effective PRMT5 inhibitors remains a pressing task.

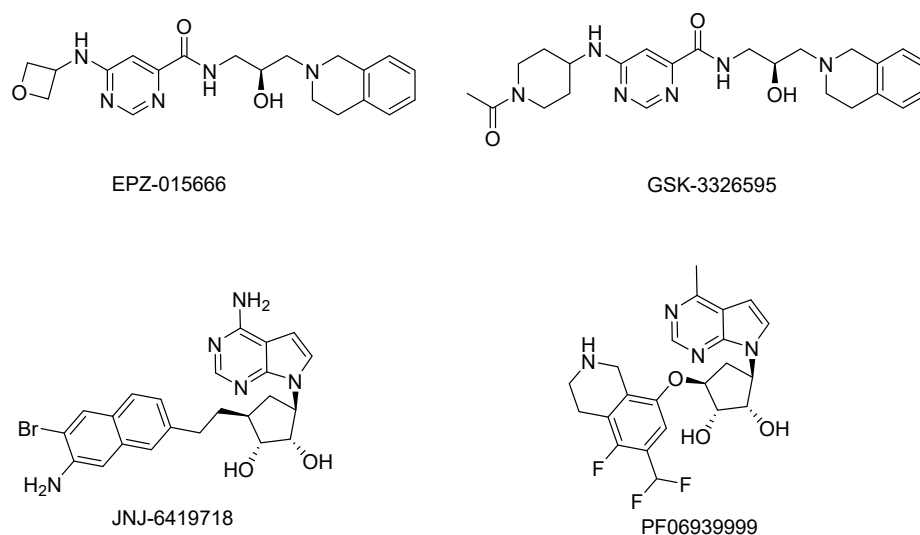


Figure 1. Chemical structures of some representative PRMT5 inhibitors.

In the present study, we present the design, synthesis and biological evaluation of a series of PRMT5 inhibitors based on the co-crystal structure of EPZ015666 and PRMT5. Among them, compound **20** displays high inhibitory activity both in enzymatic and cellular assays, which is better than GSK-3326595. Furthermore, compound **20** demonstrates potent antitumor in vivo efficacy, making further progress as a potent small molecule inhibitor targeting PRMT5.

2. Results and Discussion

2.1. Structure-Based Design of Novel PRMT5 Inhibitors

Our approach to design PRMT5 inhibitors took inspiration from the co-crystal structure of EPZ015666 and PRMT5 protein (PDB code: 4X61) (Figure 2). The computer modeling displays a key cation– π interaction between the benzene ring of THIQ and the cofactor SAM, helping to maintain high binding affinity and selectivity for PRMT5. Notably, THIQ also forms a potential π – π stacking interaction with Phe327 and the tertiary nitrogen atom of the THIQ ring system forms a key hydrogen bond, with Glu435 and Leu437 mediated by water molecule. We also noticed that the aminopyrimidine region is situated at the hydrophobic site of the substrate-binding pocket, surrounded by Tyr304, Val326, Phe327, Phe577 and Phe580. Therefore, increasing the volume of the aromatic ring in this area might

be advantageous to strengthening the π - π or/and hydrophobic interaction with residues in the active site, thereby enhancing the binding affinity between the compound and PRMT5.

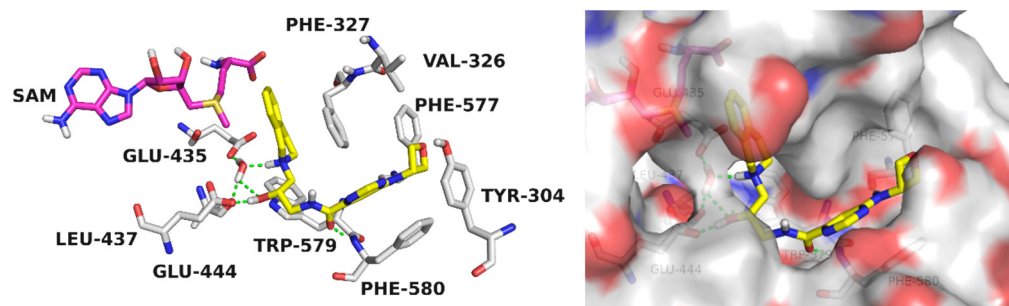


Figure 2. Crystal structure of the PRMT5–EPZ-015666 complex (PDB code: 4X61). Protein surface is shown in gray.

2.2. Evaluation of PRMT5 Enzymatic Activities

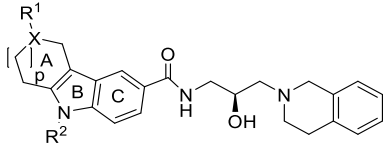
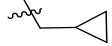
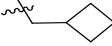
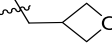
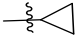
We initially attempted replacing 1-(4-(pyrimidin-4-ylamino) piperidin-1-yl) ethan-1-one with the carbazole ring. Using a radioactivity-based assay monitoring the transfer of the methyl group from ^3H -SAM to peptide substrate, we found that compound **1** displays similar PRMT5 inhibitory activity compared with GSK-3326595. However, the structure–activity study of R^1 and R^2 did not significantly improve the activity (Table 1).

Table 1. In Vitro PRMT5 Inhibitory activity of compounds 1–6.

Compound	R^1	R^2	Inhibition Rate%@100 nM	IC_{50} (nM)
 1-6				
1	H	H	73 ± 0.7	13 ± 8.9
2	Me	H	59 ± 0.4	ND
3	F	H	65 ± 0.2	ND
4	OCH_3	H	64 ± 1.5	ND
5	Cl	H	69 ± 7.0	ND
6	H	Me	63 ± 3.2	ND
GSK-3326595			77 ± 3.8	9.2 ± 0.1

It is noteworthy that the inhibitory activity could be maintained when the carbazole moiety was replaced by less rigid tetrahydrocarbazole ring, with an IC_{50} of 18.6 ± 0.9 nM (compound **7**). No dramatic change is observed in inhibitory activity upon increasing or decreasing the size of ring A. The substituent R^1 on the ring A were further investigated, and unfortunately, when R^1 is methyl or ethyl, the PRMT5 inhibitory activity of the compound **11** and **12** decreases slightly (Table 2).

Table 2. In Vitro PRMT5 Inhibitory activity of compounds 7–26.

Compound	R ¹	R ²	X	P	Inhibition Rate% @100 nM	IC ₅₀ (nM)
						
7-26						
7	H	H	C	1	75 ± 0.7	18.6 ± 0.9
8	H	H	C	0	74 ± 2.0	ND
9	H	H	C	2	73 ± 4.1	ND
10	H	H	C	3	71 ± 1.3	ND
11	Me	H	C	1	67 ± 3.5	ND
12	Et	H	C	1	58 ± 3.7	ND
13	H	Me	C	1	75 ± 0.7	10 ± 4.4
14	H	Et	C	1	81 ± 3.2	8.8 ± 0.4
15	H	<i>n</i> -Pr	C	1	79 ± 4.0	4.2 ± 2.1
16	H	<i>i</i> -Pr	C	1	70 ± 0.2	ND
17	H	<i>i</i> -Bu	C	1	75 ± 1.6	ND
18	H		C	1	60 ± 4.6	ND
19	H		C	1	80 ± 1.0	7.5 ± 0.3
20	H		C	1	83 ± 12	4.2 ± 1.3
21	Me	H	N	1	48 ± 1.2	ND
22	Et	H	N	1	64 ± 10.7	ND
23		H	N	1	52 ± 4.8	ND
24	<i>n</i> -Pr	H	N	1	63 ± 4.4	ND
25	<i>i</i> -Pr	H	N	1	51 ± 4.2	ND
26	<i>i</i> -Bu	H	N	1	59 ± 1.4	ND
GSK-3326595					77 ± 3.8	9.2 ± 0.1

Then we explored the effects of substituent R² on PRMT5 inhibition and expected to enhance the interaction between the pocket defined by Thr323, Val326 and Phe327 and target compounds by introducing different hydrophobic groups (13–20). Surprisingly, compounds with the bulkier *n*-propyl, cyclobutyl and oxetane groups yield excellent PRMT5 inhibitory activities, and compounds 15 and 20 display the most potent inhibitory activity on PRMT5 with IC₅₀ of 4.2 nM. Modeling of the binding pose of 20 was performed by manual ligand building from the crystal structure of the complex of PRMT5 and EPZ-015666 (PDB code: 4X61)(Figure 3). The result shows that the 2,3,4,9-tetrahydro-1*H*-carbazole fragment, which mimics the *N*-(oxetan-3-yl) pyrimidin-4-amine moiety in EPZ015666, is situated at the hydrophobic site of the substrate-binding pocket, and the oxetan-3-ylmethyl moiety is extended to the small hydrophobic region and undergoes a hydrogen-bonding interaction with Thr323. Finally, we investigated the effects of the tetrahydropyrido [4,3-*b*] indole moiety and its substituent R¹ on PRMT5 inhibition. However, whether the tetrahydrocarbazole moiety is replaced by tetrahydropyrido[4,3-*b*]indole or substituent R¹ is replaced by alkyl, the outcome is unfavorable for PRMT5 inhibitory activity.

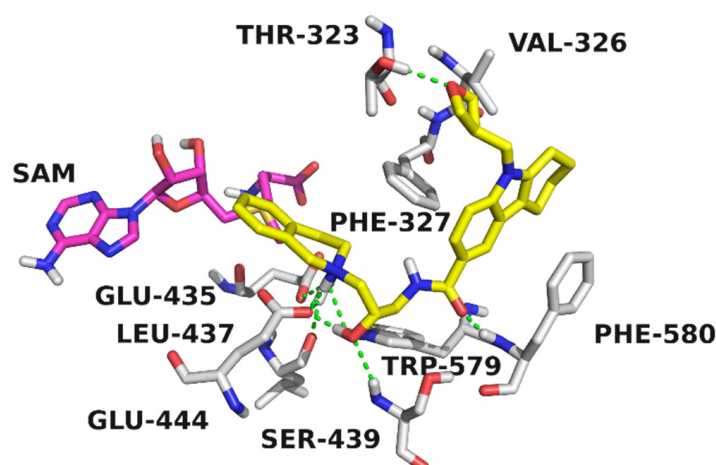


Figure 3. Compound **20** docked into X-ray structure of PRMT5 (PDB code:4X61).

2.3. In Vitro Anti-Proliferative Activity Evaluation

MV-4-11 and MDA-MB-468 cell lines were used to evaluate the anti-proliferative activities of the selected target compounds (CellTiter-Glo assay), and AML-12 hepatocytes were selected to evaluate the toxicity of the compounds. As shown in Table 3, compound **20** exhibits stronger anti-proliferative activities than **GSK-3326595** in MV-4-11 and MDA-MB-468 cell lines. However, it has almost no toxicity compared to normal AML-12 hepatocytes.

Table 3. Anti-proliferative activity of compounds in vitro.

Compound	MV4-11 (GI ₅₀ , nM)	MDA-MB-468 (GI ₅₀ , nM)	AML-12	
			Inhibition Rate% @10 μM	Inhibition Rate% @20 μM
1	271.3 ± 151.7	552.1 ± 33.0	16.7 ± 10.4	97.5 ± 0.1
7	54.1 ± 20.5	>250	46.4 ± 3.7	98.4 ± 0.7
10	42.4 ± 2.6	125.8 ± 70.9	97.9 ± 1.2	100.7 ± 0.1
13	163.1 ± 0.3	147 ± 2.5	16.3 ± 3.4	21.2 ± 2.0
14	29.7 ± 12.8	285.7 ± 5.9	−67 ± 11.3	17.7 ± 3.5
15	39.5 ± 1.9	24.9 ± 20.2	−21.5 ± 2.0	77.3 ± 1.6
19	16 ± 2.3	99.1 ± 8.3	32.9 ± 5.4	100.2 ± 0.9
20	4.6 ± 0.9	9.9 ± 6.8	−30.5 ± 9.4	−27.0 ± 1.2
GSK-3326595	9.3 ± 2.8	37.3 ± 3.0	22.9 ± 3.0	26.5 ± 2.0

2.4. Cellular Thermal Shift Assay (CETSA)

To confirm the target engagement in cells, compound **20** and **GSK-3326595** were selected and evaluated using an MV-4-11 cell line by CETSA [26,27]. As shown in Figure 4, we measured the PRMT5 melting curve and facilitated the temperature selection, as the PRMT5 melting point of **GSK-3326595** and compound **20** increased by 5.5 °C and 7.2 °C compared to the DMSO vehicle, indicating the thermal stabilization of proteins upon ligand binding. Moreover, the binding of **20** also inhibits the degradation of PRMT5 at 58 °C in a dose-dependent manner. All the results demonstrate better binding potency in a cellular context.

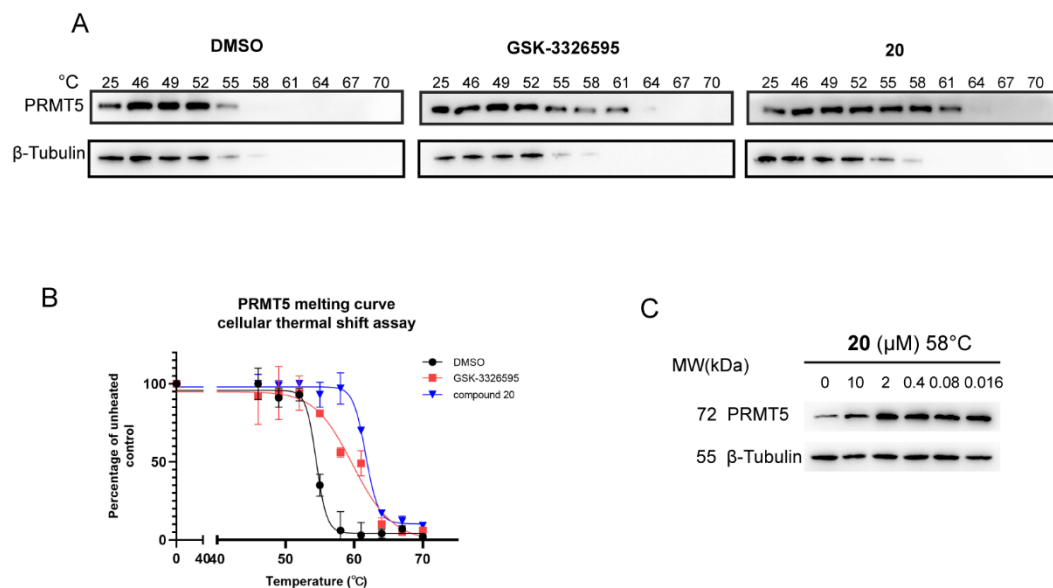


Figure 4. (A) MV-4-11 cell lines were treated for 18 h with 1 μ M GSK-3326595, and compound **20** showed stabilization of PRMT5 in cellular thermal shift analysis in whole-cell lysates. (B) The relative strength of PRMT5 signal on the Western blots was measured by densitometry. The melting temperature for PRMT5 was shifted by 5.5 $^{\circ}$ C and 7.2 $^{\circ}$ C. All data were analyzed using a Boltzmann sigmoidal fit. Each point plotted represents the mean of three replicates for each temperature; error bars denote \pm SD. (C) The binding of **20** inhibits the degradation of PRMT5 at 58 $^{\circ}$ C in a dose-dependent manner.

2.5. Characterization of Cell Methylation and Proliferation

To further evaluate if compound **20** exhibits anti-proliferative activity depending on PRMT5 inhibition, we analyzed the effect of compound **20** on PRMT5 substrate sDMA protein expression in MV-4-11 cell, with high expression in PRMT5. As shown in Figure 5, the treatment of compound **20** leads to a concentration-dependent decrease in sDMA, indicating its better PRMT5 inhibition than GSK-3326595. All the cellular data suggests that compound **20** inhibits cell proliferation through inhibiting PRMT5 activity.

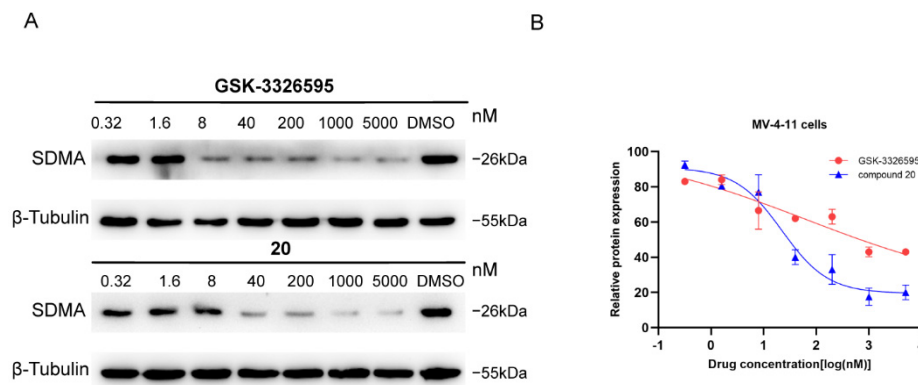


Figure 5. (A) Effect of diluent of GSK-3326595 and compound **20** by five-fold concentration gradient protein expression of MV-4-11 cancer cells. Western blot analysis of PRMT5 substrate sDMA, as indicated in MV-4-11 cancer cells treated with the indicated compounds for 96 h. β -Tubulin was used as a loading control. (B) The relative strength of sDMA signal on the Western blots was measured by densitometry. The data are shown as the mean \pm SD of three independent experiments.

2.6. In Vivo Pharmacokinetic Study

Considering the desirable enzymatic potency, as well as the potent anti-proliferative activity in several cancer cell lines, compound **20** was selected and evaluated for its pharmacokinetics (PK) data in male ICR mice at 2 mg/kg and 10 mg/kg for intravenous

(iv) and oral (po) administration, respectively. The resulting data (Tables S1 and S2) are summarized in Table 4. It reveals that compound 20 exhibits an acceptable PK profile with a $T_{1/2}$ of 6.06 h, a modest drug exposure in blood ($AUC_{0-\infty}$ values after oral treatment of 10 mg/kg are 747 h·ng/mL) and an acceptable oral bioavailability of 14.5%.

Table 4. Pharmacokinetics (PK) of Compound 20 *.

Route	Species	C_{max} (ng/mL)	$T_{1/2}$ (h)	$AUC_{0-\infty}$ (h·ng/mL)	V_{ss} (mL/kg)	CL(mL/h/kg)	F (%)
po.	mouse	1267	6.06	747			14.5
iv.	mouse	1687	0.49	1031	1346	1944	

* $n = 3$. The compound was formulated as solution in 20% HP- β -CD in saline. Dosage: 2 mg/kg for intravenous (iv) and 10 mg/kg for oral (po)administration. ICR mouse were used. The maximum drug concentration (C_{max}) was observed at $t = 5$ min, the first sampling time point after iv administration.

2.7. Antitumor Effect of 20 In Vivo

Based on the excellent enzymatic and anti-proliferative activities of compound 20 in vitro, we then evaluated antitumor activities in vivo in an MV-4-11 xenograft mouse model. GSK-3326595 and compound 20 were administered by intraperitoneal injection twice daily (BID) for 28 consecutive days. As shown in Figure 6, compound 20 demonstrates its potent antitumor efficacy at a dose of 10 mg·kg⁻¹, and the tumor suppression effect of 20 (TGI: 47.6%) is more effective than that of the positive control GSK-3326595 (TGI: 39.3%). It is noteworthy that no significant weight fluctuations were observed, and compound 20 was well-tolerated with no mortality.

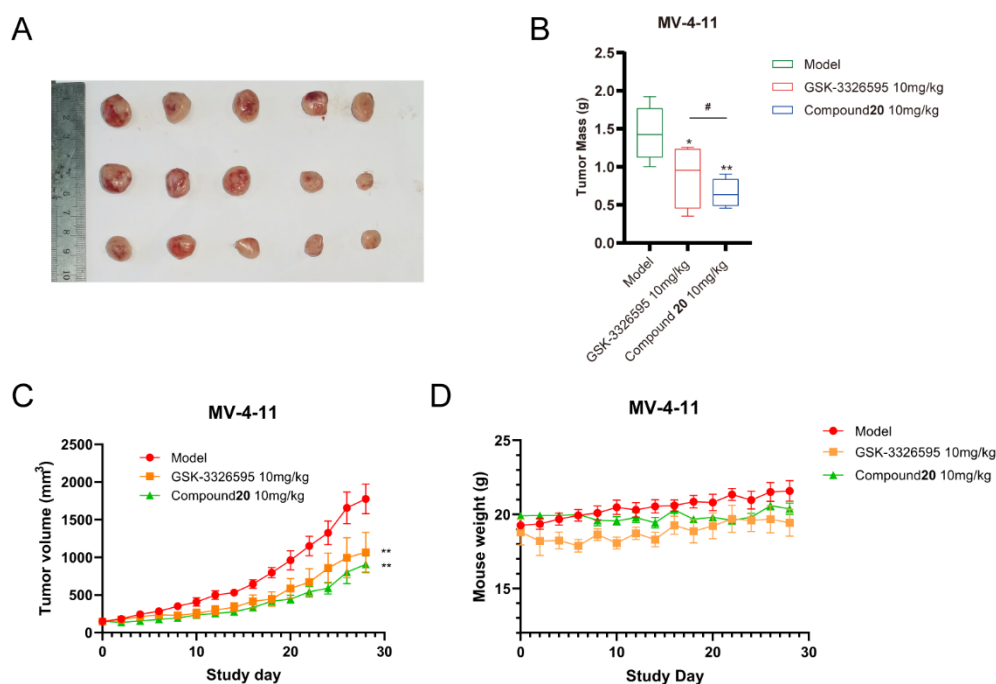


Figure 6. Effects of GSK-3326595 (10 mg·kg⁻¹, iv) and compound 20 (10 mg·kg⁻¹, iv) treatment on the tumorigenicity of MV-4-11 cells in vivo. (A) The resulting tumors excised from the animals after treatment. (B) The tumor masses for three groups of animals were compared, and each histogram represents the Mean \pm SD of 5 mice. * $p < 0.05$ vs. model, ** $p < 0.01$, # $p < 0.05$ vs. GSK-3326595. (C) The nude mouse body weight was measured every 2 days. (D) The tumor volumes of the nude mice were measured and calculated once every 2 days.

The expression of Ki-67 is positively correlated to the malignancy of tumors [28]. H&E staining shows the malignancy of the tumor and drug prognostic effect [29]. Therefore, H&E staining and Ki-67 immunohistochemistry were further used to gain insight into the

changes in the structure and appearance of cancerous cellular structures after compound 20 administration. As shown in Figure 7, all administration groups cause a decrease in the population of tumor cells, and morphological features including cell shrinkage, condensation and margination of nuclear chromatin are observed by microscopy. Meanwhile, the administration group also down-regulates the expression of Ki-67, indicating the decrease in cell proliferation.

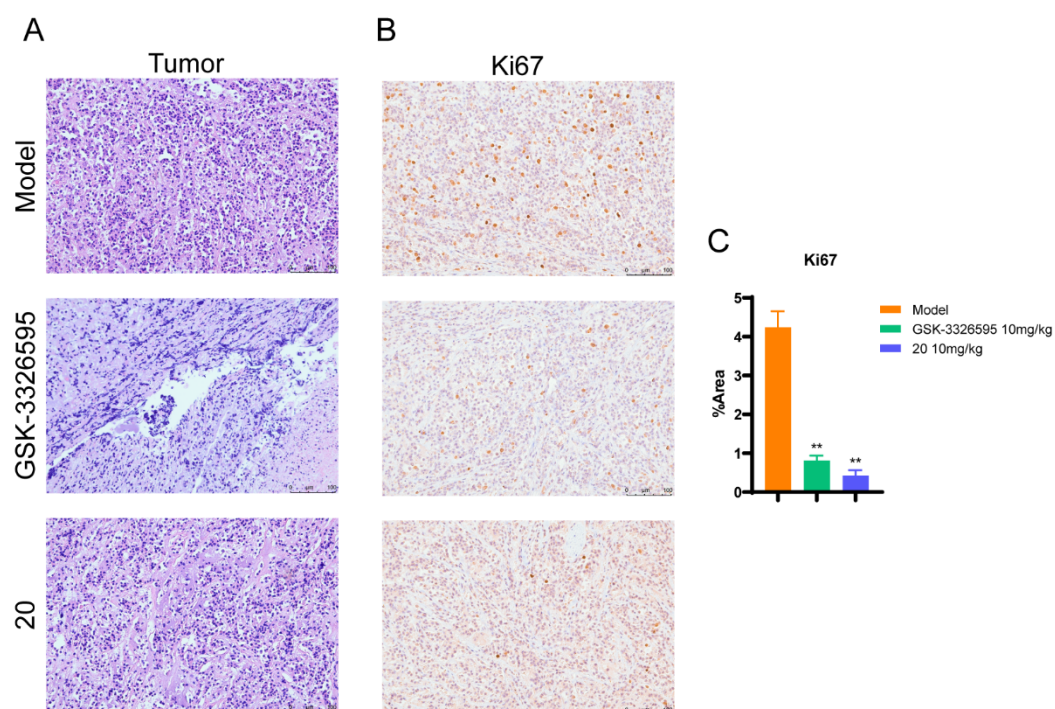


Figure 7. H&E staining and immunohistochemical analysis of Ki-67 expression in vivo. (A) Hematoxylin-eosin staining (H&E) analysis of tumor of GSK-3326595 and compound 20 treatment. (B) Immunohistochemical analysis of Ki67 in vivo. (C) Percentage of immunohistochemically stained dots. * $p < 0.05$ vs. model, ** $p < 0.01$.

2.8. Expression of sDMA In Vivo

Subsequently, we investigated the effects of compound 20 on the expression of the PRMT5 substrate sDMA in vivo (Figure 8). Similarly, the expression of sDMA was decreased after the treatment of compound 20, which was in line with its antitumor activity in vivo.

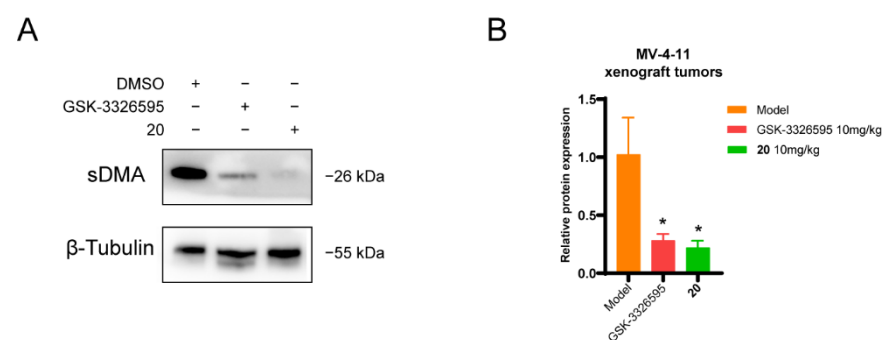
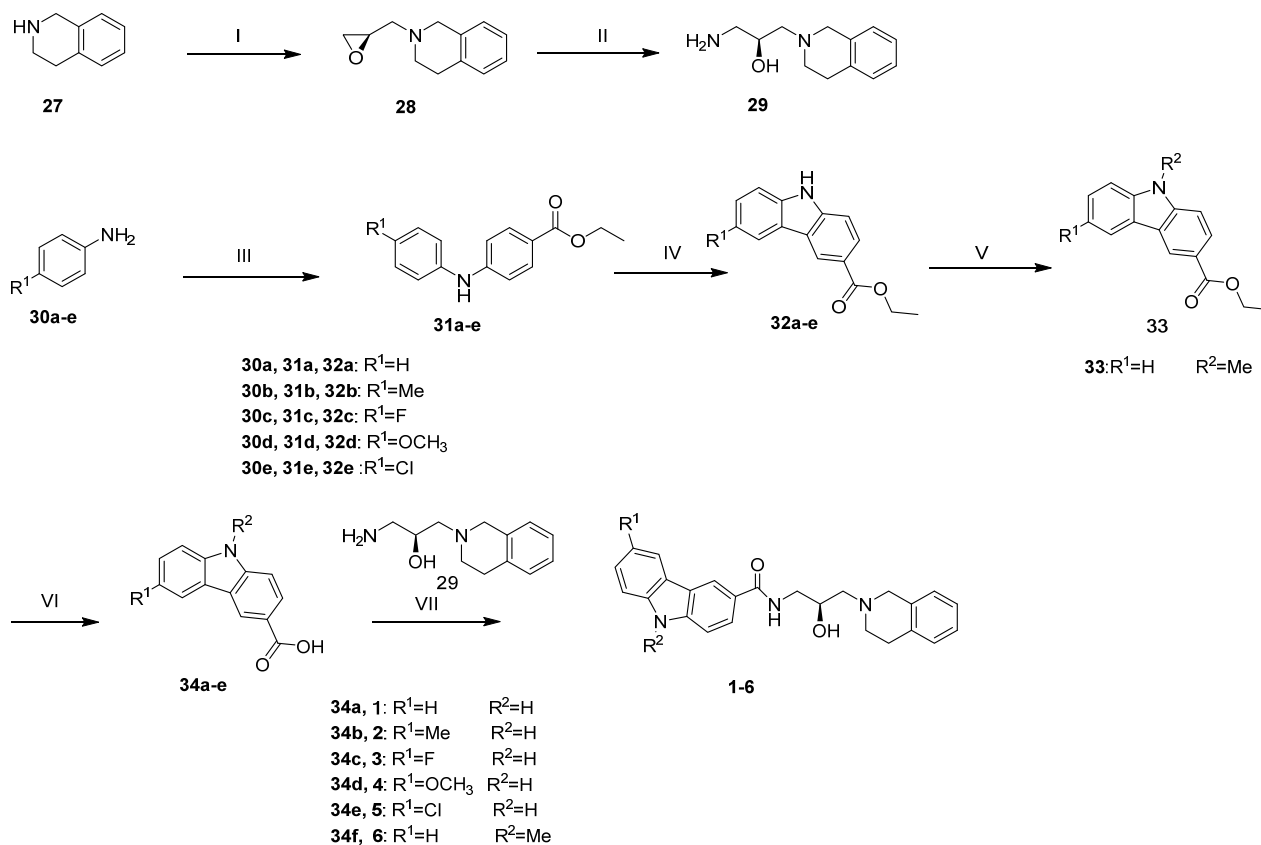


Figure 8. PRMT5 substrate sDMA expression of GSK-3326595 ($10 \text{ mg} \cdot \text{kg}^{-1}$, iv) and compound 20 ($10 \text{ mg} \cdot \text{kg}^{-1}$, iv) treatment for the tumorigenicity of MV-4-11 cells in vivo. (A) Western blot analysis of sDMA as indicated in MV-4-11 xenograft tumors treated with the indicated compounds for 28 days. (B) The relative strength of sDMA signal on the Western blots was measured by densitometry. The data are shown as the mean \pm SD of three independent experiments. * $p < 0.05$ vs. control.

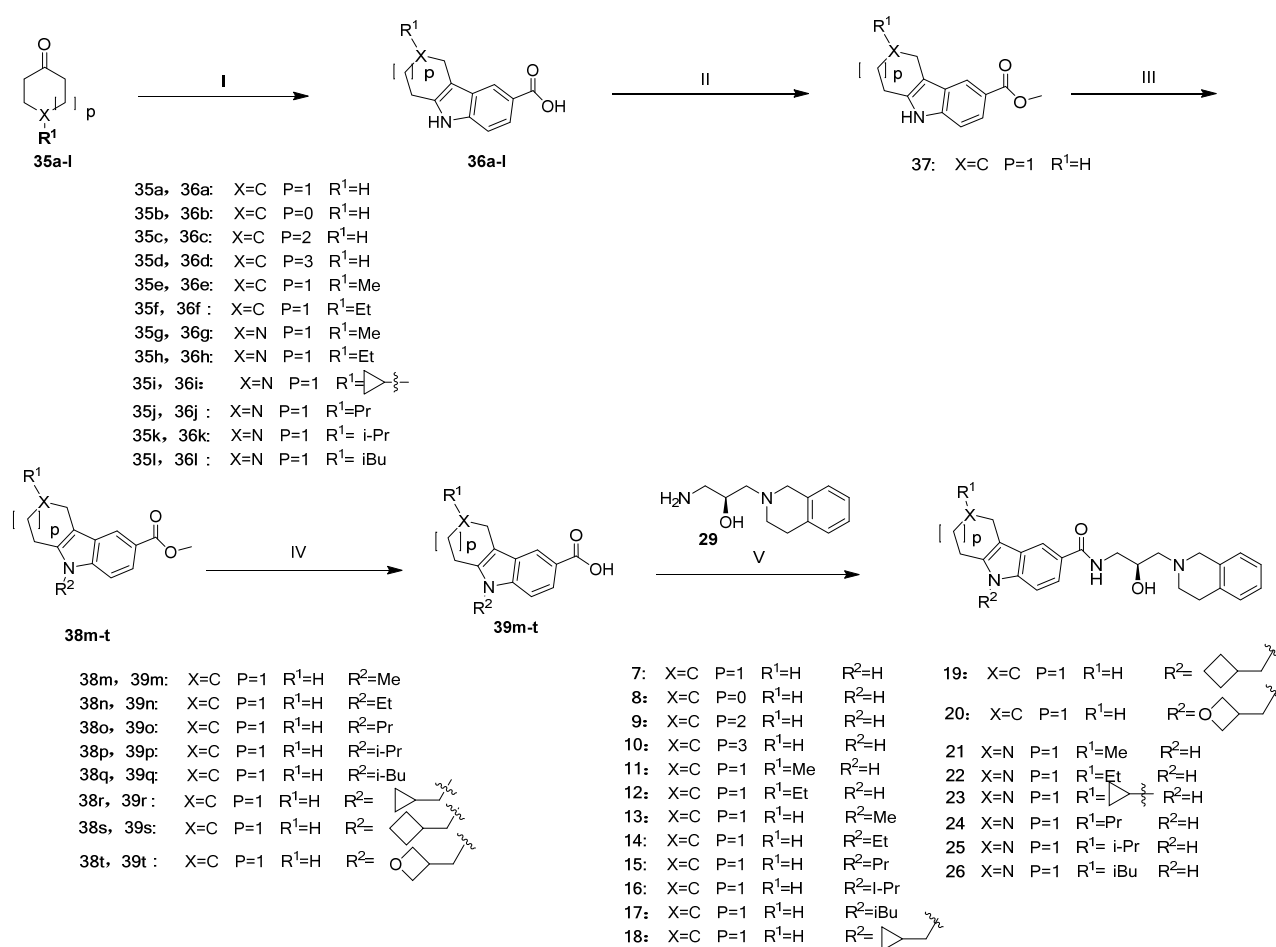
2.9. Chemistry

The preparation of compounds **1–6** was described in Scheme 1. Initially, the commercially available 1,2,3,4-tetrahydroisoquinoline was substituted by (*R*)-epichlorohydrin to afford compound **28**, which was ring-opened by ammonolysis of ammonia water to give compound **29**. Meanwhile, compounds **30a–30e** were reacted with ethyl 4-bromobenzoate to afford compounds **31a–31e**, which were catalyzed by Pd(OAc)₂ to afford compounds **32a–32e**. **32a** reacted with MeI by nucleophilic substitution to afford compound **33**. Subsequently, **32a–32e** and **33** were hydrolyzed by KOH to obtain compounds **34a–34f**. As a result, compounds **1–6** were synthesized from carboxylic acid **34a–34f** and the intermediate **29**.



Scheme 1. Reagents and conditions: (I) (*R*)-epichlorohydrin, THF, KF, 0 °C–rt; (II) NH₃H₂O, EtOH, 80 °C; (III) ethyl 4-bromobenzoate, Pd(OAc)₂, BINAP, K₂CO₃, Toluene, 120 °C; (IV) Pd(OAc)₂, AcOH, 120 °C; (V) NaH, MeI, DMF; (VI) KOH, EtOH, H₂O, 90 °C; (VII) HATU, DIEA, DCM.

The synthetic routes of compounds **7–26** were shown in Scheme 2. **35a–35l** were reacted with *p*-carboxyphenylhydrazine to afford compounds **36a–36l**, which were subsequently reacted with MeOH in the presence of H₂SO₄ to give compound **37**. R² was introduced by nucleophilic substitution using halogenated alkanes to yield compounds **38m–38t**, which were hydrolyzed by LiOH to afford compounds **39m–39t**. Finally, the target compounds **7–26** were prepared from the corresponding carboxylic acid and the key intermediates **29**.



Scheme 2. Reagents and conditions: (I) H₂SO₄, 4-hydrazinylbenzoic acid, H₂O, 100 °C; (II) H₂SO₄, MeOH, 65 °C; (III) NaH, halogenated alkane, DMF, 0-r.t.; (IV) KOH, EtOH, H₂O, 90 °C; (V) HATU, DIEA, DCM.

3. Experimental Sections

3.1. General Chemistry

All solvents and reagents were purchased from commercial vendors and used without further purification. The progress of the reaction was monitored by TLC on pre-coated silica gel plates (silica gel 60 F254), and spots were observed by UV light (λ_{\max} = 254 or 365 nm) or other suitable stain. ¹H (300 or 400 MHz) and ¹³C NMR (75 MHz or 101 MHz) spectra were recorded by Bruker spectrometer with TMS as internal standard. Coupling constants (J) are expressed in hertz (Hz). Ordinary and high-resolution mass spectra were obtained by ESI-MS. The purification of compounds was conducted by flash column chromatography (silica gel 200–300 mesh). The purity of all target compounds was > 95%, as determined by HPLC (BDS Hypersil C18, λ = 254 nm).

3.1.1. General Procedure for the Synthesis of Compounds 28 and 29

(R)-2-(oxiran-2-ylmethyl)-1,2,3,4-tetrahydroisoquinoline (28).

To a mixture of 27 (1.00 g, 7.50 mmol) in THF (10 mL) at 0 °C was successively added KF (0.87 g, 15 mmol) and (S)-oxiran-2-ylmethyl 3-nitrobenzenesulfonate (2.20 g, 15 mmol). The reaction mixture was stirred at 0 °C for 1 h, and then reacted at 25 °C for 16 h. The mixture was filtered to remove the solid, and washed with THF (5 mL) twice. The filtrate was concentrated and purified by column chromatography (PE/EA: 5/1) to obtain 0.86 g of pale-yellow oil with a yield of 61.0%; ¹H NMR (300 MHz, Chloroform-*d*) δ 7.15–7.08 (m, 3 H), 7.06–7.01 (m, 1 H), 3.86–3.66 (m, 2 H), 3.25–3.17 (m, 1 H), 2.99–2.87 (m, 4 H), 2.86–2.76 (m, 2 H), 2.56 (dd, *J* = 5.0, 2.7 Hz, 1 H), 2.50–2.40 (m, 1 H); MS (ESI): 190.1.

(S)-1-amino-3-(3,4-dihydroisoquinolin-2(1H)-yl) propan-2-ol (**29**).

A mixture of **28** (1.00 g, 26.0 mmol) in NH₄OH (10 mL) was refluxed at 80 °C for 3 h. The reaction mixture was allowed to cool to 25 °C and concentrated under reduced pressure. The crude product was purified using column chromatography (DCM/MeOH: 15/1) to obtain the titled compound (0.37 g, 34.0%) as a pale-yellow oil; ¹H NMR (400 MHz, Chloroform-*d*) δ 7.18–7.09 (m, 3 H), 7.05–6.98 (m, 1 H), 3.85–3.76 (m, 2 H), 3.62 (d, *J* = 14.9 Hz, 1 H), 2.97–2.81 (m, 4 H), 2.78–2.64 (m, 2 H), 2.61–2.46 (m, 2 H); MS (ESI): 207.1.

3.1.2. General Procedure for the Synthesis of Compound **31a–e**

A mixture of **30a–e** (2.80 mmol, 1 eq), ethyl 4-bromobenzoate (2.80 mmol, 1 eq), Pd(OAc)₂ (0.14 mmol, 0.05 eq), BINAP (0.14 mmol, 0.05 eq) and K₂CO₃ (3.0 mmol, 1.07 eq) in toluene (10 mL) was refluxed under an atmosphere of N₂ for 6 h. The reaction mixture was allowed to cool to rt and concentrated under reduced pressure. The crude product was purified using a column chromatography cation to obtain compound **31a–e**.

Ethyl 4-(phenylamino) benzoate (**31a**).

White solid; yield: 83.6%; ¹H NMR (300 MHz, Chloroform-*d*) δ 7.99–7.92 (m, 2 H), 7.40–7.32 (m, 2 H), 7.24–7.18 (m, 2 H), 7.13–7.05 (m, 1 H), 7.05–6.99 (m, 2 H), 6.07 (s, 1 H), 4.37 (q, *J* = 7.1 Hz, 2 H), 1.40 (t, *J* = 7.1 Hz, 2 H); MS (ESI): 242.1.

Ethyl 4-(*p*-tolylamino) benzoate (**31b**).

White solid; yield: 59.5%; ¹H NMR (300 MHz, Chloroform-*d*) δ 7.95–7.89 (m, 2 H), 7.20–7.14 (m, 2 H), 7.13–7.07 (m, 3 H), 6.97–6.91 (m, 2 H), 4.35 (q, *J* = 7.1 Hz, 2 H), 2.36 (s, 3 H), 1.39 (t, *J* = 7.1 Hz, 3 H); MS (ESI): 256.1.

Ethyl 4-((4-fluorophenyl) amino) benzoate (**31c**).

White solid; yield: 81.4%; ¹H NMR (300 MHz, Chloroform-*d*) δ 7.95 (d, *J* = 8.2 Hz, 2 H), 7.20 (d, *J* = 4.9 Hz, 1 H), 7.18 (d, *J* = 4.6 Hz, 1 H), 7.08 (t, *J* = 8.4 Hz, 2 H), 6.93 (d, *J* = 8.2 Hz, 2 H), 4.38 (q, *J* = 6.9 Hz, 2 H), 1.42 (t, *J* = 7.1 Hz, 3 H); MS (ESI): 260.1.

Ethyl 4-((4-methoxyphenyl) amino) benzoate (**31d**).

White solid; yield: 90.8%; ¹H NMR (300 MHz, Chloroform-*d*) δ 7.90 (d, *J* = 8.8 Hz, 2 H), 7.16 (d, *J* = 8.7 Hz, 2 H), 7.00–6.89 (m, 2 H), 6.84 (d, *J* = 8.7 Hz), 4.35 (q, *J* = 7.1 Hz, 2 H), 3.84 (s, 2 H), 1.39 (t, *J* = 7.1 Hz, 3 H); MS (ESI): 272.1.

Ethyl 4-((4-chlorophenyl) amino) benzoate (**31e**).

White solid; yield: 84.8%; ¹H NMR (300 MHz, Chloroform-*d*) δ 8.03–7.89 (m, 2 H), 7.31–7.27 (m, 2 H), 7.12–7.06 (m, 2 H), 6.99–6.93 (m, 2 H), 4.34 (q, *J* = 7.1 Hz, 2 H), 1.38 (t, *J* = 7.1 Hz, 3 H); MS (ESI): 276.1.

3.1.3. General Procedure for the Synthesis of Compound **32a–e**

A mixture of **31a–e** (1.24 mmol, 1 eq), Pd(OAc)₂ (1.37 mmol, 1 eq) in AcOH (8 mL) was refluxed under an atmosphere of N₂ for 1 h. The reaction mixture was allowed to cool to rt and concentrated under reduced pressure. The crude product was purified using a column chromatography cation to obtain compound **32a–e**.

Ethyl 9*H*-carbazole-3-carboxylate (**32a**).

White solid; yield: 64.0%; ¹H NMR (300 MHz, Chloroform-*d*) δ 8.85 (d, *J* = 1.4 Hz, 1 H), 8.43 (s, 1 H), 8.21–8.10 (m, 2 H), 7.51–7.42 (m, 3 H), 7.35–7.30 (m, 1 H), 4.48 (q, *J* = 7.1 Hz, 2 H), 1.49 (t, *J* = 7.1 Hz, 3 H); MS (ESI): 240.1. Ethyl 6-methyl-9*H*-carbazole-3-carboxylate (**32b**).

White solid; yield: 55.0%; ¹H NMR (300 MHz, DMSO-*d*₆) δ 11.56 (s, 1 H), 8.80 (s, 1 H), 7.98 (dd, *J* = 8.6, 1.6 Hz, 1 H), 7.95–7.81 (m, 1 H), 7.51 (d, *J* = 8.6 Hz, 1 H), 7.45 (d, *J* = 8.8 Hz, 1 H), 7.07 (dd, *J* = 8.8, 2.5 Hz, 1 H), 4.35 (q, *J* = 7.1 Hz, 2 H), 3.87 (s, 3 H), 1.37 (t, *J* = 7.1 Hz, 3 H); MS (ESI): 254.1.

Ethyl 6-fluoro-9*H*-carbazole-3-carboxylate (**32c**).

White solid; yield: 52.0%; ¹H NMR (300 MHz, DMSO-*d*₆) δ 11.82 (s, 1 H), 8.85 (s, 1 H), 8.17 (dd, *J* = 9.4, 2.5 Hz, 1 H), 8.06 (dd, *J* = 9.4, 2.4 Hz, 1 H), 7.63–7.54 (m, 2 H), 7.37–7.30 (m, 1 H), 4.38 (q, *J* = 7.1 Hz, 2 H), 1.40 (t, *J* = 7.1 Hz, 3 H); MS (ESI): 258.1.

Ethyl 6-methoxy-9*H*-carbazole-3-carboxylate (**32d**).

White solid; yield: 68.5%; MS (ESI): 270.1.

Ethyl 6-chloro-9H-carbazole-3-carboxylate (32e).

White solid; yield: 80.6%; $^1\text{H NMR}$ (300 MHz, DMSO-*d*₆) δ 11.92 (s, 1 H), 8.88 (s, 1 H), 8.43 (d, $J = 2.0$ Hz, 1 H), 8.07 (dd, $J = 8.6, 1.7$ Hz, 1 H), 7.59 (dd, $J = 8.6, 5.3$ Hz, 2 H), 7.48 (dd, $J = 8.6, 2.0$ Hz, 1 H), 4.38 (q, $J = 7.1$ Hz, 2 H), 1.40 (t, $J = 7.1$ Hz, 3 H); MS (ESI): 274.1.

3.1.4. General Procedure for the Synthesis of Compound 33

32a (300 mg, 1.31 mmol) in DMF (5 mL) was stirred at 0 °C for 5 min. NaH (90 mg, 3.75 mmol) was added and reacted at 25 °C for 0.5 h, MeI (264 mg, 1.86 mmol) was added dropwise at 0 °C, followed by reaction at 25 °C for 3 h TLC (DCM/MeOH: 50/1) to monitor the completion of the reaction. H₂O (20 mL) was added to quench the reaction. EA (10 mL \times 3) extracted with EA (10 mL \times 3), washed with saturated NaCl (10 mL), dried over anhydrous Na₂SO₄, filtrated, and the filtrate was dried and purified by column chromatography (DCM/MeOH: 50/1) to obtain the titled compound (45 mg, 47.3%) as a white solid; MS (ESI): 254.1.

3.1.5. General Procedure for the Synthesis of Compounds 34a–f

A mixture of **32a–e** or **33** (0.38 mmol, 1 eq), KOH (1.13 mmol, 3 eq) in EtOH (5 mL) and H₂O (1 mL) was refluxed under an atmosphere of N₂ for 3 h. The reaction mixture was allowed to cool to rt and concentrated under reduced pressure. 5 mL H₂O was added, 1 mL 2N (HCL) was added to adjust the pH to about 3, and suction filtration to obtain the compounds **34a–f**.

9H-carbazole-3-carboxylic acid (34a).

White solid; yield: 86.1%; MS (ESI):212.1.

6-methyl-9H-carbazole-3-carboxylic acid (34b).

White solid; yield: 81.8%; $^1\text{H NMR}$ (300 MHz, DMSO-*d*₆) δ 11.58 (s, 1 H), 8.70 (d, $J = 1.5$ Hz, 1 H), 8.01 (s, 1 H), 7.97 (dd, $J = 8.5, 1.7$ Hz, 1 H), 7.50 (d, $J = 8.5$ Hz, 1 H), 7.43 (d, $J = 8.2$ Hz, 1 H), 7.26 (dd, $J = 8.3, 1.3$ Hz, 1 H), 2.47 (s, 3 H); MS (ESI): 226.1.

6-fluoro-9H-carbazole-3-carboxylic acid (34c).

White solid; yield: 56.3%; $^1\text{H NMR}$ (300 MHz, DMSO-*d*₆) δ 12.63 (s, 1 H), 11.75 (s, 1 H), 8.82 (s, 1 H), 8.12 (dd, $J = 9.4, 2.6$ Hz, 1 H), 8.02 (dd, $J = 8.6, 1.7$ Hz, 1 H), 7.54 (dd, $J = 8.8, 4.7$ Hz, 2 H), 7.34–7.24 (m, 1 H); MS (ESI): 230.1.

6-methoxy-9H-carbazole-3-carboxylic acid (34d).

White solid; yield: 86.5%; $^1\text{H NMR}$ (300 MHz, DMSO-*d*₆) δ 11.52 (s, 1 H), 8.80 (s, 1 H), 7.99 (d, $J = 8.6$ Hz, 1 H), 7.86 (s, 1 H), 7.53–7.43 (m, 2 H), 7.09 (d, $J = 11.2$ Hz, 1 H), 3.88 (s, 3 H); MS (ESI): 242.1.

6-chloro-9H-carbazole-3-carboxylic acid (34e).

White solid; yield: 88.7%; $^1\text{H NMR}$ (300 MHz, DMSO-*d*₆) δ 11.90 (s, 1 H), 8.86 (s, 1 H), 8.40 (d, $J = 2.0$ Hz, 1 H), 8.06 (dd, $J = 8.5, 1.6$ Hz, 1 H), 7.60 (s, 1 H), 7.57 (s, 1 H), 7.47 (dd, $J = 8.6, 2.0$ Hz, 1 H); MS (ESI): 246.0.

9-methyl-9H-carbazole-3-carboxylic acid (34f).

White solid; yield: 75.0%; $^1\text{H NMR}$ (300 MHz, DMSO-*d*₆) δ 12.5 (s, 1 H), 8.82 (d, $J = 1.5$ Hz, 1 H), 8.31 (d, $J = 7.7$ Hz, 1 H), 8.10 (dd, $J = 8.6, 1.7$ Hz, 1 H), 7.71 (d, $J = 3.9$ Hz, 1 H), 7.56 (t, $J = 7.7$ Hz, 1 H), 7.30 (t, $J = 7.4$ Hz, 1 H), 3.96 (s, 3 H). MS (ESI): 226.1.

3.1.6. General Procedure for the Synthesis of Compounds 36a–l

A mixture of **35a–l** (6.49 mmol, 1.3 eq), 4-hydrazinylbenzoic acid (5.00 mmol, 1 eq) in 10% H₂SO₄ (20 mL) was refluxed under an atmosphere of N₂ for 3 h. The reaction mixture was allowed to cool to rt the solid was precipitated and filtrated, and the filter cake with 10 mL of H₂O, and dried to obtain the compound **36a–l**.

2,3,4,9-tetrahydro-1H-carbazole-6-carboxylic acid (36a).

Gray solid; yield: 75.0%; $^1\text{H NMR}$ (300 MHz, DMSO-*d*₆) δ 12.32 (s, 1 H), 11.08 (s, 1 H), 8.04 (s, 1 H), 7.66 (dd, $J = 8.5, 1.6$ Hz, 1 H), 7.31 (d, $J = 8.5$ Hz, 1 H), 2.80–2.60 (m, 4 H), 1.96–1.76 (m, 4 H); MS (ESI): 216.1.

1,2,3,4-tetrahydrocyclopenta[b]indole-7-carboxylic acid (36b).

Gray solid; yield: 68.0%; ^1H NMR (300 MHz, DMSO-*d*₆) δ 11.24 (s, 1 H), 8.03 (s, 1 H), 7.66 (dd, $J = 8.5, 1.6$ Hz, 1 H), 7.36 (d, $J = 8.5$ Hz, 1 H), 2.86 (t, $J = 7.0$ Hz, 2 H), 2.79 (t, $J = 6.9$ Hz, 2 H), 2.49–2.30 (m, 2 H); MS (ESI): 202.1.

5,6,7,8,9,10-hexahydrocyclohepta[*b*]indole-2-carboxylic acid (36c).

Gray solid; yield: 97.8%; ^1H NMR (300 MHz, DMSO-*d*₆) δ 11.11 (s, 1 H), 8.07 (s, 1 H), 7.64 (d, $J = 8.3$ Hz, 1 H), 7.30 (d, $J = 8.4$ Hz, 1 H), 2.85 (t, $J = 5.6$ Hz, 2 H), 2.78 (t, $J = 5.6$ Hz, 2 H), 1.93–1.82 (m, 2 H), 1.79–1.64 (m, 4 H); MS (ESI): 230.1.

6,7,8,9,10,11-hexahydro-5*H*-cycloocta[*b*]indole-2-carboxylic acid (36d).

Gray solid; yield: 56.3%; ^1H NMR (400 MHz, DMSO-*d*₆) δ 12.32 (s, 1 H), 11.08 (s, 1 H), 8.06 (s, 1 H), 7.62 (d, $J = 10.0$ Hz, 1 H), 7.29 (d, $J = 8.5$ Hz, 1 H), 2.83 (q, $J = 5.6$ Hz, 4 H), 1.80–1.58 (m, 4 H), 1.52–1.29 (m, 4 H); MS (ESI): 243.1.

3-methyl-2,3,4,9-tetrahydro-1*H*-carbazole-6-carboxylic acid (36e).

Gray solid; yield: 90.2%; ^1H NMR (400 MHz, DMSO-*d*₆) δ 11.07 (s, 1 H), 8.01 (s, 1 H), 7.63 (dd, $J = 8.5, 1.6$ Hz, 1 H), 7.28 (d, $J = 8.4$ Hz, 1 H), 2.84–2.76 (m, 1 H), 2.77–2.71 (m, 2 H), 2.22 (dd, $J = 15.3, 9.5$ Hz, 1 H), 1.97–1.82 (m, 2 H), 1.58–1.43 (m, 1 H), 1.10 (d, $J = 6.5$ Hz, 3 H); MS (ESI): 230.1.

3-ethyl-2,3,4,9-tetrahydro-1*H*-carbazole-6-carboxylic acid (36f).

Gray solid; yield: 78.6%; ^1H NMR (400 MHz, DMSO-*d*₆) δ 11.06 (s, 1 H), 8.03 (s, 1 H), 7.63 (dd, $J = 8.4, 1.7$ Hz, 1 H), 7.28 (dd, $J = 8.6, 1.4$ Hz, 1 H), 2.84 (dd, $J = 15.4, 4.9$ Hz, 1 H), 2.77–2.69 (m, 2 H), 2.22 (dd, $J = 14.7, 10.0$ Hz, 2 H), 1.97 (dd, $J = 11.5, 6.1$ Hz, 1 H), 1.72–1.59 (m, 1 H), 1.55–1.37 (m, 3 H), 0.99 (t, $J = 7.3$ Hz, 3 H); MS (ESI): 244.1.

2-methyl-2,3,4,5-tetrahydro-1*H*-pyrido[4,3-*b*] indole-8-carboxylic acid (36g).

White solid; yield: 8.85%; ^1H NMR (300 MHz, DMSO-*d*₆) δ 11.79 (s, 1 H), 11.45 (s, 1 H), 8.11 (s, 1 H), 7.73 (dd, $J = 8.6, 1.5$ Hz, 1 H), 7.42 (d, $J = 8.5$ Hz, 1 H), 4.63 (d, $J = 13.0$ Hz, 1 H), 4.29 (dd, $J = 14.3, 7.3$ Hz, 1 H), 3.74–3.62 (m, 1 H), 3.54–3.40 (m, 1 H), 3.33–3.19 (m, 1 H), 3.11–2.98 (m, 1 H), 2.93 (d, $J = 4.3$ Hz, 3 H); MS (ESI): 231.1.

2-ethyl-2,3,4,5-tetrahydro-1*H*-pyrido[4,3-*b*] indole-8-carboxylic acid (36h).

White solid; yield: 8.35%; ^1H NMR (300 MHz, DMSO-*d*₆) δ 8.20 (d, $J = 1.5$ Hz, 1 H), 7.75 (dd, $J = 8.6, 1.5$ Hz, 1 H), 7.45 (d, $J = 8.6$ Hz, 1 H), 4.72 (d, $J = 14.5$ Hz, 1 H), 4.30 (d, $J = 14.5$ Hz, 1 H), 3.83–3.73 (m, 1 H), 3.50–3.40 (m, 1 H), 3.39–3.28 (m, 2 H), 3.28–3.18 (m, 1 H), 3.17–3.00 (m, 1 H), 1.40 (t, $J = 7.2$ Hz, 3 H); MS (ESI): 245.1.

2-cyclopropyl-2,3,4,5-tetrahydro-1*H*-pyrido[4,3-*b*] indole-8-carboxylic acid (36i).

White solid; yield: 19.41%; ^1H NMR (400 MHz, DMSO-*d*₆) δ 11.67 (s, 1 H), 11.17 (s, 1 H), 8.18 (s, 1 H), 7.72 (dd, $J = 8.5, 1.5$ Hz, 1 H), 7.40 (d, $J = 8.5$ Hz, 1 H), 4.70 (d, $J = 14.1$ Hz, 1 H), 4.46 (d, $J = 9.9$ Hz, 1 H), 3.83–3.71 (m, 1 H), 3.69–3.59 (m, 1 H), 3.32–3.20 (m, 1 H), 3.08 (d, $J = 14.8$ Hz, 1 H), 1.27 (s, 2 H), 0.92–0.78 (m, 2 H); MS (ESI): 257.1.

2-propyl-2,3,4,5-tetrahydro-1*H*-pyrido[4,3-*b*] indole-8-carboxylic acid (36j).

White solid; yield: 9.97%; ^1H NMR (300 MHz, DMSO-*d*₆) δ 11.79 (s, 1 H), 11.33 (s, 1 H), 8.19 (s, 1 H), 7.75 (dd, $J = 8.6, 1.4$ Hz, 1 H), 7.42 (s, 1 H), 4.69 (d, $J = 14.2$ Hz, 1 H), 4.31 (dd, $J = 14.6, 7.2$ Hz, 1 H), 3.80–3.68 (m, 1 H), 3.37–3.27 (m, 2 H), 3.25–3.14 (m, 2 H), 3.14–3.00 (m, 1 H), 2.02–1.80 (m, 2 H), 0.98 (t, $J = 7.3$ Hz, 3 H); MS (ESI): 259.1.

2-isopropyl-2,3,4,5-tetrahydro-1*H*-pyrido[4,3-*b*] indole-8-carboxylic acid (36k).

White solid; yield: 44.5%; ^1H NMR (300 MHz, DMSO-*d*₆) δ 11.66 (s, 1 H), 10.87 (s, 1 H), 8.20 (s, 1 H), 7.72 (d, $J = 10.1$ Hz, 1 H), 7.41 (d, $J = 8.5$ Hz, 1 H), 4.60–4.49 (m, 1 H), 4.33 (dd, $J = 14.6, 8.8$ Hz, 1 H), 3.78–3.61 (m, 1 H), 3.34–3.20 (m, 2 H), 3.10–2.93 (m, 1 H), 1.40 (dd, $J = 10.8, 6.6$ Hz, 6 H); MS (ESI): 259.1.

2-isobutyl-2,3,4,5-tetrahydro-1*H*-pyrido[4,3-*b*] indole-8-carboxylic acid (36l).

White solid; yield: 23.5%; ^1H NMR (300 MHz, DMSO-*d*₆) δ 8.21 (d, $J = 1.5$ Hz, 1 H), 7.75 (dd, $J = 8.6, 1.7$ Hz, 1 H), 7.45 (d, $J = 8.6$ Hz, 1 H), 4.75 (d, $J = 14.6$ Hz, 1 H), 4.35 (d, $J = 14.7$ Hz, 1 H), 3.83–3.73 (m, 1 H), 3.54–3.48 (m, 1 H), 3.48–3.40 (m, 1 H), 3.34–3.19 (m, 1 H), 3.18–3.11 (m, 1 H), 3.10–3.02 (m, 1 H), 2.36–2.21 (m, 1 H), 1.03 (t, $J = 6.9$ Hz, 6 H); MS (ESI): 273.2.

3.1.7. General Procedure for the Synthesis of Compound 37

Methyl 2,3,4,9-tetrahydro-1*H*-carbazole-6-carboxylate (**37**).

A mixture of **36a** (2.2 g, 10.22 mmol) in MeOH (40 mL) and H₂SO₄ (2.19 mL, 40.88 mmol) was refluxed at 65 °C for 6 h. The reaction mixture was allowed to cool to rt and concentrated under reduced pressure. H₂O (30 mL) was added, extracted with EA (10 mL × 3), washed with saturated NaCl (10 mL), dried with anhydrous Na₂SO₄, filtrate, and dried to obtain the titled compound (2.3 g, 98.3%) as a white solid; ¹H NMR (300 MHz, Chloroform-*d*) δ 8.22 (s, 1 H), 7.95 (s, 1 H), 7.83 (d, *J* = 8.5 Hz, 1 H), 7.25 (d, *J* = 8.5 Hz, 1 H), 3.93 (s, 3 H), 2.72 (t, *J* = 5.9 Hz, 4 H), 1.97–1.81 (m, 4 H); MS (ESI): 230.1.

3.1.8. General Procedure for the Synthesis of Compounds 38m–t

37 (1.31 mmol, 1 eq) in DMF (5 mL) was stirred at 0 °C for 5 min, NaH (2.62 mmol, 2 eq) was added and reacted at 25 °C for 0.5 h, halogenated alkane (2.62 mmol, 2 eq) was added dropwise at 0 °C, followed by a reaction at 25 °C for 3 h TLC (DCM/MeOH: 50/1) to monitor the completion of the reaction. H₂O (20 mL) was added to quench the reaction, extracted with EA (10 mL × 3), washed with saturated NaCl (10 mL), dried over anhydrous Na₂SO₄ filtrate, the filtrate was dried and purified by column chromatography to obtain compound **38m–t**.

methyl 9-methyl-2,3,4,9-tetrahydro-1*H*-carbazole-6-carboxylate (**38m**).

White solid; yield: 98.6%; ¹H NMR (300 MHz, Chloroform-*d*) δ 8.26 (d, *J* = 1.4 Hz, 1 H), 7.89 (dd, *J* = 8.6, 1.6 Hz, 1 H), 7.26 (d, *J* = 8.6 Hz, 1 H), 3.95 (s, 3 H), 3.65 (s, 3 H), 2.80–2.70 (m, 4 H), 2.04–1.83 (m, 4 H); MS (ESI): 244.1.

methyl 9-ethyl-2,3,4,9-tetrahydro-1*H*-carbazole-6-carboxylate (**38n**).

White solid; yield: 13.4%; ¹H NMR (300 MHz, DMSO-*d*₆) δ 8.09 (s, 1 H), 7.73 (d, *J* = 8.5 Hz, 1 H), 7.49 (d, *J* = 8.5 Hz, 1 H), 4.16 (q, *J* = 7.0 Hz, 2 H), 3.86 (s, 3 H), 2.83–2.65 (m, 4 H), 2.03–1.76 (m, 4 H), 1.26 (t, *J* = 6.8 Hz, 3 H); MS (ESI): 258.1.

methyl 9-propyl-2,3,4,9-tetrahydro-1*H*-carbazole-6-carboxylate (**38o**).

White solid; yield: 94.4%; MS (ESI): 272.2.

Methyl 9-isopropyl-2,3,4,9-tetrahydro-1*H*-carbazole-6-carboxylate (**38p**).

White solid; yield: 18.0%; ¹H NMR (400 MHz, DMSO-*d*₆) δ 8.04 (d, *J* = 1.5 Hz, 1 H), 7.67 (dd, *J* = 8.7, 1.7 Hz, 1 H), 7.58 (d, *J* = 8.7 Hz, 1 H), 4.76–4.59 (m, 1 H), 3.84 (s, 2 H), 2.77 (t, *J* = 5.8 Hz, 2 H), 2.66 (t, *J* = 5.8 Hz, 2 H), 1.92–1.83 (m, 2 H), 1.83–1.73 (m, 2 H), 1.51 (d, *J* = 7.0 Hz, 6 H); MS (ESI): 272.2.

Methyl 9-isobutyl-2,3,4,9-tetrahydro-1*H*-carbazole-6-carboxylate (**38q**).

White solid; yield: 32.1%; ¹H NMR (400 MHz, DMSO-*d*₆) δ 8.06 (d, *J* = 1.4 Hz, 1 H), 7.69 (dd, *J* = 8.6, 1.7 Hz, 1 H), 7.46 (d, *J* = 8.6 Hz, 1 H), 3.89 (d, *J* = 7.6 Hz, 2 H), 3.83 (s, 3 H), 2.76–2.66 (m, 4 H), 2.13–2.01 (m, 1 H), 1.92–1.74 (m, 4 H), 0.85 (d, *J* = 6.7 Hz, 6 H); MS (ESI): 286.2.

Methyl 9-(cyclopropylmethyl)-2,3,4,9-tetrahydro-1*H*-carbazole-6-carboxylate (**38r**).

White solid; yield: 60.7%; MS (ESI): 284.2.

Methyl 9-(cyclobutylmethyl)-2,3,4,9-tetrahydro-1*H*-carbazole-6-carboxylate (**38s**).

White solid; yield: 7.71%; ¹H NMR (300 MHz, DMSO-*d*₆) δ 8.05 (d, *J* = 1.7 Hz, 1 H), 7.69 (dd, *J* = 8.6, 1.7 Hz, 1 H), 7.51 (d, *J* = 8.6 Hz, 1 H), 4.12 (d, *J* = 7.1 Hz, 2 H), 3.83 (s, 3 H), 2.79–2.66 (m, 5 H), 1.93–1.71 (m, 10 H); MS (ESI): 298.2.

methyl 9-(oxetan-3-ylmethyl)-2,3,4,9-tetrahydro-1*H*-carbazole-6-carboxylate (**38t**).

White solid; yield: 5.67%; ¹H NMR (300 MHz, DMSO-*d*₆) δ 12.38 (s, 1 H), 8.06 (d, *J* = 1.2 Hz, 1 H), 7.71 (dd, *J* = 8.6, 1.5 Hz, 1 H), 7.43 (d, *J* = 8.6 Hz, 1 H), 3.65 (s, 3 H), 2.86–2.62 (m, 4 H), 2.03–1.73 (m, 4 H); MS (ESI): 230.1.

3.1.9. General Procedure for the Synthesis of Compounds 39m–t

9-methyl-2,3,4,9-tetrahydro-1*H*-carbazole-6-carboxylic acid (**39m**).

White solid; yield: 91.9%; ¹H NMR (300 MHz, DMSO-*d*₆) δ 12.38 (s, 1 H), 8.06 (d, *J* = 1.2 Hz, 1 H), 7.71 (dd, *J* = 8.6, 1.5 Hz, 1 H), 7.43 (d, *J* = 8.6 Hz, 1 H), 3.65 (s, 3 H), 2.86–2.62 (m, 4 H), 2.03–1.73 (m, 4 H); MS (ESI): 230.1.

9-ethyl-2,3,4,9-tetrahydro-1*H*-carbazole-6-carboxylic acid (**39n**).

White solid; yield: 79.2%; ^1H NMR (400 MHz, DMSO-*d*₆) δ 12.34 (s, 1 H), 8.04 (d, $J = 1.2$ Hz, 1 H), 7.69 (dd, $J = 8.6, 1.6$ Hz, 1 H), 7.43 (d, $J = 8.6$ Hz, 1 H), 4.13 (q, $J = 7.1$ Hz, 2 H), 2.73 (t, $J = 5.6$ Hz, 2 H), 2.67 (t, $J = 5.5$ Hz, 2 H), 1.93–1.75 (m, 4 H), 1.23 (t, $J = 7.1$ Hz, 3 H); MS (ESI): 244.1.

9-propyl-2,3,4,9-tetrahydro-1*H*-carbazole-6-carboxylic acid (**39o**).

White solid; yield: 85.1%; ^1H NMR (300 MHz, DMSO-*d*₆) δ 12.39 (s, 1 H), 8.07 (d, $J = 1.6$ Hz, 1 H), 7.71 (dd, $J = 8.6, 1.4$ Hz, 1 H), 7.46 (d, $J = 8.6$ Hz, 1 H), 4.06 (t, $J = 7.2$ Hz, 2 H), 2.81–2.63 (m, 4 H), 1.96–1.76 (m, 4 H), 1.75–1.60 (m, 2 H), 0.88 (t, $J = 7.4$ Hz, 3 H); MS (ESI): 258.1.

9-isobutyl-2,3,4,9-tetrahydro-1*H*-carbazole-6-carboxylic acid (**39p**).

White solid; yield: 62.1%; ^1H NMR (300 MHz, DMSO-*d*₆) δ 8.09 (d, $J = 1.6$ Hz, 1 H), 7.72 (dd, $J = 8.7, 1.4$ Hz, 1 H), 7.62 (d, $J = 8.7$ Hz, 1 H), 4.81–4.69 (m, 1 H), 2.83 (t, $J = 5.0$ Hz, 1 H), 2.73 (t, $J = 5.0$ Hz, 2 H), 2.02–1.90 (m, 2 H), 1.90–1.79 (m, 2 H), 1.58 (d, $J = 6.9$ Hz, 6 H); MS (ESI): 258.1.

9-isobutyl-2,3,4,9-tetrahydro-1*H*-carbazole-6-carboxylic acid (**39q**).

White solid; yield: 95.3%; ^1H NMR (300 MHz, DMSO-*d*₆) δ 8.06 (d, $J = 1.5$ Hz, 1 H), 7.70 (dd, $J = 8.6, 1.7$ Hz, 1 H), 7.45 (d, $J = 8.7$ Hz, 1 H), 3.91 (d, $J = 7.5$ Hz, 2 H), 2.79–2.69 (m, 4 H), 2.15–2.00 (m, 1 H), 1.95–1.76 (m, 4 H), 0.88 (d, $J = 6.6$ Hz, 6 H); MS (ESI): 272.2.

9-(cyclopropylmethyl)-2,3,4,9-tetrahydro-1*H*-carbazole-6-carboxylic acid (**39r**).

White solid; yield: 87.7%; ^1H NMR (300 MHz, DMSO-*d*₆) δ 8.06 (d, $J = 1.5$ Hz, 1 H), 7.70 (dd, $J = 8.6, 1.4$ Hz, 1 H), 7.49 (d, $J = 8.6$ Hz, 1 H), 4.02 (d, $J = 6.7$ Hz, 2 H), 2.84–2.64 (m, 4 H), 1.97–1.75 (m, 4 H), 1.24–1.08 (m, 1 H), 0.54–0.43 (m, 2 H), 0.43–0.33 (m, 2 H); MS (ESI): 270.1.

9-(cyclobutylmethyl)-2,3,4,9-tetrahydro-1*H*-carbazole-6-carboxylic acid (**39s**).

White solid; yield: 65.4%; ^1H NMR (300 MHz, DMSO-*d*₆) δ 8.05 (d, $J = 1.6$ Hz, 1 H), 7.70 (dd, $J = 8.6, 1.7$ Hz, 1 H), 7.50 (d, $J = 8.6$ Hz, 1 H), 4.14 (d, $J = 7.0$ Hz, 2 H), 2.80–2.60 (m, 5 H), 2.00–1.69 (m, 10 H); MS (ESI): 284.2.

9-(oxetan-3-ylmethyl)-2,3,4,9-tetrahydro-1*H*-carbazole-6-carboxylic acid (**39t**).

White solid; yield: 59.4%; MS (ESI): 286.1.

3.1.10. General Procedure for the Synthesis of Target Products 1–26

A mixture of **34a–f** or **36a–l** or **39m–t** (0.30 mmol, 1 eq), **29** (0.30 mmol, 1 eq), HATU (0.30 mmol, 1 eq), DIPEA (0.75 mmol, 2.5 eq) in DCM (2 mL) was stirred under an atmosphere of N₂ for 3 h. The reaction mixture was concentrated under reduced pressure and purified by column chromatography (DCM + 5% Ammonium hydroxide) to obtain the titled compounds **1–26**.

(*S*)-*N*-(3-(3,4-dihydroisoquinolin-2(1*H*)-yl)-2-hydroxypropyl)-9*H*-carbazole-3-carboxamide (**1**).

White solid; yield: 25.2%; HPLC Purity: 97.6%; ^1H NMR (300 MHz, Methanol-*d*₄) δ 8.63 (s, 1 H), 8.05 (d, $J = 7.8$ Hz, 1 H), 7.88 (d, $J = 8.5$ Hz, 1 H), 7.55–7.37 (m, 3 H), 7.22 (t, $J = 7.4$ Hz, 1 H), 7.16–7.06 (m, 3 H), 7.05–6.98 (m, 1 H), 4.25–4.12 (m, 1 H), 3.76 (s, 2 H), 3.68–3.51 (m, 2 H), 2.98–2.80 (m, 4 H), 2.79–2.62 (m, 2 H); ^{13}C NMR (75 MHz, Methanol-*d*₄) δ 170.06, 142.09, 140.65, 133.62, 128.29, 126.26, 126.12, 126.05, 125.51, 124.57, 124.07, 122.79, 122.68, 119.89, 119.44, 119.24, 110.81, 110.17, 67.12, 62.25, 56.05, 51.25, 45.07, 28.14; HRMS (ESI+): m/z calcd for C₂₅H₂₆N₃O₂ 400.2025 [M + H]⁺; found: 400.2014.

(*S*)-*N*-(3-(3,4-dihydroisoquinolin-2(1*H*)-yl)-2-hydroxypropyl)-6-methyl-9*H*-carbazole-3-carboxamide (**2**).

White solid; yield: 50.0%; HPLC Purity: 98.8%; ^1H NMR (300 MHz, Methanol-*d*₄) δ 8.61 (d, $J = 1.6$ Hz, 1 H), 7.90 (s, 1 H), 7.87–7.82 (m, 1 H), 7.41 (s, 1 H), 7.38 (s, 1 H), 7.31–7.25 (m, 1 H), 7.16–7.10 (m, 3 H), 7.10–7.04 (m, 1 H), 4.25–4.15 (m, 1 H), 3.80 (s, 2 H), 3.69–3.50 (m, 2 H), 3.00–2.87 (m, 4 H), 2.83–2.37 (m, 2 H), 2.54 (s, 3 H); ^{13}C NMR (75 MHz, Methanol-*d*₄) δ 170.05, 142.37, 138.92, 133.82, 133.58, 128.47, 128.23, 127.29, 126.21, 126.10, 125.48, 124.33, 123.90, 123.03, 122.54, 119.61, 119.41, 110.42, 109.90, 67.11, 56.07, 51.30, 44.94, 28.16, 20.15; HRMS (ESI+): m/z calcd for C₂₆H₂₈N₃O₂ 414.2182 [M + H]⁺; found: 414.2170.

(*S*)-*N*-(3-(3,4-dihydroisoquinolin-2(1*H*)-yl)-2-hydroxypropyl)-6-fluoro-9*H*-carbazole-3-carboxamide (**3**).

White solid; yield: 47.5%; HPLC Purity: 97.7%; ^1H NMR (300 MHz, Methanol-*d*₄) δ 8.60 (d, *J* = 1.4 Hz, 1 H), 7.93–7.87 (m, 1 H), 7.81–7.74 (m, 1 H), 7.51–7.46 (m, 1 H), 7.45–7.41 (m, 1 H), 7.27–7.19 (m, 1 H), 7.17–7.09 (m, 3 H), 7.09–7.03 (m, 1 H), 4.26–4.14 (m, 1 H), 3.79 (s, 2 H), 3.69–3.52 (m, 2 H), 2.99–2.83 (m, 4 H), 2.82–2.60 (m, 2 H); ^{13}C NMR (75 MHz, Methanol-*d*₄) δ 169.73, 143.05, 137.02, 134.14, 133.72, 128.22, 126.18, 126.02, 125.42, 125.09, 124.28, 119.78, 113.72, 113.38, 111.58, 111.46, 110.31, 105.40, 105.09, 67.14, 62.43, 56.21, 51.39, 45.06, 28.36; HRMS (ESI⁺): *m/z* calcd for C₂₅H₂₅FN₃O₂ 418.1931 [M + H]⁺; found: 418.1919.

(*S*)-*N*-(3-(3,4-dihydroisoquinolin-2(1*H*)-yl)-2-hydroxypropyl)-6-methoxy-9*H*-carbazole-3-carboxamide (4).

White solid; yield: 60.8%; HPLC Purity: 97.4%; ^1H NMR (300 MHz, Methanol-*d*₄) δ 8.62 (s, 1 H), 7.84 (d, *J* = 8.6 Hz, 1 H), 7.64 (d, *J* = 2.1 Hz, 1 H), 7.39 (t, *J* = 8.3 Hz, 2 H), 7.16–7.06 (m, 3 H), 7.04–6.98 (m, 1 H), 4.23–4.13 (m, 1 H), 3.91 (s, 3 H), 3.75 (s, 2 H), 3.69–3.50 (m, 2 H), 2.96–2.82 (m, 4 H), 2.79–2.64 (m, 2 H); ^{13}C NMR (75 MHz, Methanol-*d*₄) δ 170.09, 153.90, 142.70, 135.52, 133.92, 133.62, 128.25, 126.24, 126.08, 125.47, 124.40, 123.61, 123.27, 119.63, 115.30, 111.56, 110.21, 102.72, 67.23, 62.13, 56.03, 55.22, 51.23, 44.96, 28.13; HRMS (ESI⁺): *m/z* calcd for C₂₆H₂₈N₃O₃ 430.2131 [M + H]⁺; found: 430.2118.

(*S*)-6-chloro-*N*-(3-(3,4-dihydroisoquinolin-2(1*H*)-yl)-2-hydroxypropyl)-9*H*-carbazole-3-carboxamide (5).

White solid; yield: 66.7%; HPLC Purity: 97.7%; ^1H NMR (400 MHz, Methanol-*d*₄) δ 8.59 (d, *J* = 1.4 Hz, 1 H), 8.07 (d, *J* = 2.0 Hz, 1 H), 7.91–7.86 (m, 1 H), 7.50–7.39 (m, 3 H), 7.15–7.09 (m, 3 H), 7.09–7.02 (m, 1 H), 4.23–4.15 (m, 1 H), 3.79 (s, 2 H), 3.67–3.49 (m, 2 H), 2.97–2.87 (m, 4 H), 2.77–2.66 (m, 2 H); ^{13}C NMR (75 MHz, DMSO-*d*₆) δ 167.37, 142.32, 139.18, 134.44, 128.87, 126.85, 126.47, 126.31, 126.19, 125.97, 125.86, 124.34, 123.91, 121.54, 120.92, 120.33, 113.28, 111.06, 67.38, 62.88, 56.43, 51.61, 45.47, 29.00; HRMS (ESI⁺): *m/z* calcd for C₂₅H₂₅ClN₃O₂ 434.1635 [M + H]⁺; found: 434.1627.

(*S*)-*N*-(3-(3,4-dihydroisoquinolin-2(1*H*)-yl)-2-hydroxypropyl)-9-methyl-9*H*-carbazole-3-carboxamide (6).

White solid; yield: 45.4%; HPLC Purity: 99.6%; ^1H NMR (300 MHz, Methanol-*d*₄) δ 8.57 (d, *J* = 1.8 Hz, 1 H), 8.00 (d, *J* = 7.7 Hz, 1 H), 7.94–7.87 (m, 1 H), 7.57–7.40 (m, 2 H), 7.32 (d, *J* = 8.6 Hz, 1 H), 7.27–7.18 (m, 1 H), 7.14–7.03 (m, 3 H), 7.04–6.92 (m, 1 H), 4.24–4.10 (m, 1 H), 3.75 (s, 3 H), 3.71 (s, 2 H), 3.67–3.52 (m, 2 H), 2.90–2.80 (m, 4 H), 2.71 (m, 2 H); ^{13}C NMR (75 MHz, Methanol-*d*₄) δ 169.66, 142.70, 141.56, 134.14, 133.72, 128.24, 126.20, 126.07, 125.98, 125.48, 125.41, 124.71, 124.26, 122.51, 122.23, 119.87, 119.32, 108.65, 107.89, 79.04, 67.13, 62.46, 56.18, 51.34, 45.12, 37.50, 36.44, 27.95; HRMS (ESI⁺): *m/z* calcd for C₂₆H₂₈N₃O₂ 414.2182 [M + H]⁺; found: 414.2167.

(*S*)-*N*-(3-(3,4-dihydroisoquinolin-2(1*H*)-yl)-2-hydroxypropyl)-2,3,4,9-tetrahydro-1*H*-carbazole-6-carboxamide (7).

White solid; yield: 48.1%; HPLC Purity: 99.8%; ^1H NMR (300 MHz, Methanol-*d*₄) δ 7.96 (s, 1 H), 7.52 (d, *J* = 8.5 Hz, 1 H), 7.22 (d, *J* = 8.5 Hz, 1 H), 7.18–7.06 (m, 3 H), 7.07–7.00 (m, 1 H), 4.21–4.08 (m, 1 H), 3.76 (s, 2 H), 3.64–3.48 (m, 2 H), 2.99–2.82 (m, 4 H), 2.80–2.62 (m, 6 H), 2.00–1.82 (m, 4 H); ^{13}C NMR (75 MHz, Methanol-*d*₄) δ 170.94, 138.13, 136.21, 133.80, 133.61, 128.30, 127.39, 126.30, 126.15, 125.55, 123.62, 119.34, 116.96, 109.96, 109.84, 67.14, 62.16, 56.00, 51.18, 44.97, 28.04, 23.01, 22.88, 22.62, 20.41; HRMS (ESI⁺): *m/z* calcd for C²⁵H³⁰N³O² 404.2338 [M + H]⁺; found: 404.2326.

(*S*)-*N*-(3-(3,4-dihydroisoquinolin-2(1*H*)-yl)-2-hydroxypropyl)-1,2,3,4-tetrahydrocyclopenta[*b*]indole-7-carboxamide (8).

White solid; yield: 47.6%; HPLC Purity: 98.7%; ^1H NMR (400 MHz, Methanol-*d*₄) δ 7.91 (d, *J* = 1.5 Hz, 1 H), 7.51–7.45 (m, 1 H), 7.26 (d, *J* = 8.6 Hz, 1 H), 7.16–7.08 (m, 3 H), 7.08–6.98 (m, 1 H), 4.21–4.10 (m, 1 H), 3.76 (s, 2 H), 3.60–3.47 (m, 2 H), 2.96–2.90 (m, 2 H), 2.90–2.85 (m, 4 H), 2.84–2.79 (m, 2 H), 2.76–2.64 (m, 2 H), 2.63–2.50 (m, 2 H); ^{13}C NMR (75 MHz, Methanol-*d*₄) δ 170.95, 146.13, 143.32, 133.70, 133.56, 128.33, 126.32, 126.20, 125.59, 124.11, 124.04, 119.24, 118.78, 117.65, 111.02, 67.11, 62.00, 55.90, 51.09, 44.91, 28.25, 27.94, 25.10, 23.73; HRMS (ESI⁺): *m/z* calcd for C₂₄H₂₈N₃O₂ 390.2182 [M + H]⁺; found: 390.2172.

(S)-N-(3-(3,4-dihydroisoquinolin-2(1H)-yl)-2-hydroxypropyl)-5,6,7,8,9,10-hexahydrocyclohepta[b]indole-2-carboxamide (**9**).

White solid; yield: 50.1%; HPLC Purity: 97.5%; ^1H NMR (300 MHz, Methanol-*d*₄) δ 8.00 (d, *J* = 1.7 Hz, 1 H), 7.50–7.45 (m, 1 H), 7.20 (d, *J* = 8.5 Hz, 1 H), 7.15–7.09 (m, 3 H), 7.07–7.01 (m, 1 H), 4.23–4.10 (m, 1 H), 3.77 (s, 2 H), 3.66–3.46 (m, 2 H), 2.98–2.80 (m, 8 H), 2.79–2.59 (m, 2 H), 2.01–1.89 (m, 2 H), 1.88–1.70 (m, 4 H); ^{13}C NMR (75 MHz, Methanol-*d*₄) δ 171.02, 136.68, 133.44, 133.44, 128.68, 128.30, 126.28, 126.25, 125.61, 123.64, 118.89, 116.97, 113.66, 67.08, 61.89, 55.88, 51.16, 44.80, 31.68, 28.62, 27.87, 24.22; HRMS (ESI+): *m/z* calcd for C₂₆H₃₂N₃O₂ 418.2495 [M + H]⁺; found: 418.2483.

(S)-N-(3-(3,4-dihydroisoquinolin-2(1H)-yl)-2-hydroxypropyl)-6,7,8,9,10,11-hexahydro-5H-cycloocta[b]indole-2-carboxamide (**10**).

White solid; yield: 51.3%; HPLC Purity: 97.0%; ^1H NMR (300 MHz, Methanol-*d*₄) δ 8.03 (s, 1 H), 7.54–7.47 (m, 1 H), 7.23 (d, *J* = 8.5 Hz, 1 H), 7.20–7.10 (m, 3 H), 7.10–7.03 (m, 1 H), 4.24–4.12 (m, 1 H), 3.79 (s, 2 H), 3.66–3.46 (m, 2 H), 3.01–2.84 (m, 8 H), 2.80–2.65 (m, 2 H), 1.87–1.70 (m, 4 H), 1.58–1.41 (m, 4 H); ^{13}C NMR (75 MHz, Methanol-*d*₄) δ 170.95, 137.78, 137.52, 133.96, 133.67, 128.26, 127.95, 126.25, 126.08, 125.48, 123.70, 118.95, 116.99, 111.69, 109.82, 67.28, 62.18, 56.10, 51.28, 44.89, 29.80, 29.27, 28.17, 25.62, 25.59, 24.96, 21.62; HRMS (ESI+): *m/z* calcd for C₂₇H₃₄N₃O₂ 432.2651 [M + H]⁺; found: 432.2639.

N-((S)-3-(3,4-dihydroisoquinolin-2(1H)-yl)-2-hydroxypropyl)-3-methyl-2,3,4,9-tetrahydro-1H-carbazole-6-carboxamide (**11**).

White solid; yield: 45.9%; HPLC Purity: 97.7%; ^1H NMR (300 MHz, Methanol-*d*₄) δ 7.96 (s, 1 H), 7.55–7.49 (m, 1 H), 7.22 (d, *J* = 8.5 Hz, 1 H), 7.19–7.10 (m, 3 H), 7.09–7.03 (m, 1 H), 4.27–4.10 (m, 1 H), 3.80 (s, 2 H), 3.66–3.48 (m, 2 H), 2.99–2.87 (m, 4 H), 2.86–2.78 (m, 3 H), 2.77–2.65 (m, 2 H), 2.35–2.20 (m, 1 H), 2.08–1.90 (m, 2 H), 1.68–1.51 (m, 1 H), 1.18 (d, *J* = 6.5 Hz, 3 H); ^{13}C NMR (75 MHz, Methanol-*d*₄) δ 170.90, 138.46, 135.87, 133.86, 133.62, 128.27, 127.29, 126.26, 126.12, 125.51, 123.68, 119.29, 116.93, 109.88, 109.74, 62.19, 56.05, 51.23, 44.93, 31.14, 29.53, 28.91, 28.11, 22.25, 20.75; HRMS (ESI+): *m/z* calcd for C₂₆H₃₂N₃O₂ 418.2495 [M + H]⁺; found: 418.2483.

N-((S)-3-(3,4-dihydroisoquinolin-2(1H)-yl)-2-hydroxypropyl)-3-ethyl-2,3,4,9-tetrahydro-1H-carbazole-6-carboxamide (**12**).

White solid; yield: 41.1%; HPLC Purity: 99.0%; ^1H NMR (300 MHz, Methanol-*d*₄) δ 7.97 (s, 1 H), 7.52 (d, *J* = 8.5 Hz, 1 H), 7.22 (d, *J* = 8.4 Hz, 1 H), 7.20–7.10 (m, 3 H), 7.10–7.02 (m, 1 H), 4.17 (m, 1 H), 3.79 (s, 2 H), 3.64–3.48 (m, 2 H), 2.99–2.83 (m, 5 H), 2.83–2.67 (m, 4 H), 2.33–2.19 (m, 1 H), 2.13–2.02 (m, 1 H), 1.80–1.64 (m, 1 H), 1.55 (m, 3 H), 1.07 (t, *J* = 7.4 Hz, 3 H); ^{13}C NMR (75 MHz, Methanol-*d*₄) δ 170.93, 138.47, 136.16, 133.80, 133.60, 128.28, 127.37, 126.28, 126.15, 125.54, 123.65, 119.30, 116.93, 109.93, 109.68, 62.11, 56.01, 51.20, 36.46, 28.99, 28.65, 28.05, 26.61, 22.32, 10.85; HRMS (ESI+): *m/z* calcd for C₂₇H₃₄N₃O₂ 432.2651 [M + H]⁺; found: 432.2639.

(S)-N-(3-(3,4-dihydroisoquinolin-2(1H)-yl)-2-hydroxypropyl)-9-methyl-2,3,4,9-tetrahydro-1H-carbazole-6-carboxamide (**13**).

White solid; yield: 57.6%; HPLC Purity: 99.1%; ^1H NMR (300 MHz, Methanol-*d*₄) δ 7.98 (s, 1 H), 7.63–7.57 (m, 1 H), 7.25 (d, *J* = 8.6 Hz, 1 H), 7.19–7.08 (m, 3 H), 7.08–7.02 (m, 1 H), 4.23–4.11 (m, 1 H), 3.78 (s, 2 H), 3.64 (s, 3 H), 3.62–3.50 (m, 2 H), 2.98–2.84 (m, 4 H), 2.80–2.65 (m, 6 H), 2.04–1.83 (m, 4 H); ^{13}C NMR (75 MHz, Methanol-*d*₄) δ 170.90, 138.75, 133.57, 133.53, 128.34, 126.83, 126.34, 126.24, 125.63, 123.59, 119.30, 117.08, 109.93, 108.03, 67.04, 62.01, 55.89, 51.13, 44.93, 28.10, 27.88, 22.79, 21.46, 20.47; HRMS (ESI+): *m/z* calcd for C₂₆H₃₂N₃O₂ 418.2495 [M + H]⁺; found: 418.2484.

(S)-N-(3-(3,4-dihydroisoquinolin-2(1H)-yl)-2-hydroxypropyl)-9-ethyl-2,3,4,9-tetrahydro-1H-carbazole-6-carboxamide (**14**).

White solid; yield: 46.7%; HPLC Purity: 97.4%; ^1H NMR (400 MHz, Methanol-*d*₄) δ 7.94 (d, *J* = 1.6 Hz, 1 H), 7.56–7.52 (m, 1 H), 7.19 (d, *J* = 8.6 Hz, 1 H), 7.12–7.02 (m, 3 H), 7.00–6.97 (m, 1 H), 4.14–4.08 (m, 1 H), 4.05 (q, *J* = 7.3 Hz, 2 H), 3.68 (s, 2 H), 3.58–3.46 (m, 2 H), 2.88–2.82 (m, 2 H), 2.81–2.78 (m, 2 H), 2.71–2.60 (m, 6 H), 1.95–1.87 (m, 2 H), 1.86–1.78 (m, 2 H), 1.24 (t, *J* = 7.2 Hz, 3 H); ^{13}C NMR (75 MHz, Methanol-*d*₄) δ 170.55, 137.62, 134.18, 133.76, 128.21, 126.21, 125.39, 123.84, 119.35, 110.07, 107.91, 67.19, 62.46,

56.21, 51.34, 45.01, 37.50, 37.00, 28.37, 22.92, 21.46, 20.54, 14.33; HRMS (ESI+): m/z calcd for $C_{27}H_{34}N_3O_2$ 432.2651[M + H]⁺; found: 432.2638.

N-((2*R*)-2-hydroxy-3-(1,2,3,4-tetrahydronaphthalen-2-yl)propyl)-9-propyl-2,3,4,9-tetrahydro-1*H*-carbazole-6-carboxamide (**15**).

White solid; yield: 50.2%; HPLC Purity: 97.0%; ¹H NMR (300 MHz, Methanol-*d*₄) δ 7.94 (d, *J* = 1.7 Hz, 1 H), 7.55–7.49 (m, 1 H), 7.14 (d, *J* = 8.6 Hz, 1 H), 7.11–6.99 (m, 3 H), 6.99–6.91 (m, 1 H), 4.14–4.04 (m, 1 H), 3.92 (t, *J* = 7.2 Hz, 2 H), 3.65 (s, 2 H), 3.59–3.44 (m, 2 H), 2.88–2.80 (m, 2 H), 2.77–2.71 (m, 2 H), 2.69–2.55 (m, 6 H), 1.94–1.75 (m, 4 H), 1.74–1.57 (m, 2 H), 1.1–1.01 (m, 2 H), 0.85 (t, *J* = 7.4 Hz, 3 H); ¹³C NMR (75 MHz, Methanol-*d*₄) δ 170.55, 137.62, 134.18, 133.76, 128.21, 126.21, 125.39, 123.84, 119.35, 110.07, 107.91, 67.19, 62.46, 56.21, 51.34, 45.01, 37.50, 37.00, 28.37, 22.92, 21.46, 20.54, 14.33; HRMS (ESI+): m/z calcd for $C_{29}H_{37}N_2O_2$ 446.2855 [M + H]⁺; found: 446.2796.

(*S*)-*N*-(3-(3,4-dihydroisoquinolin-2(1*H*)-yl)-2-hydroxypropyl)-9-isopropyl-2,3,4,9-tetrahydro-1*H*-carbazole-6-carboxamide (**16**).

White solid; yield: 40.5%; HPLC Purity: 99.2%; ¹H NMR (300 MHz, DMSO-*d*₆) δ 8.41 (t, *J* = 5.1 Hz, 1 H), 7.97 (s, 1 H), 7.59–7.40 (m, 2 H), 7.17–7.09 (m, 3 H), 7.09–7.02 (m, 1 H), 4.99 (s, 1 H), 4.73–4.60 (m, 1 H), 4.04–3.92 (m, 1 H), 3.69 (s, 2 H), 3.33–3.24 (m, 2 H), 2.87–2.74 (m, 6 H), 2.68–2.56 (m, 4 H), 1.95–1.72 (m, 4 H), 1.52 (d, *J* = 6.9 Hz, 6 H); ¹³C NMR (101 MHz, DMSO-*d*₆) δ 167.98, 136.78, 136.38, 135.29, 134.52, 128.86, 127.45, 126.84, 126.38, 125.91, 124.76, 119.93, 117.65, 110.07, 67.46, 56.53, 51.65, 46.71, 45.56, 38.70, 29.10, 23.47, 23.09, 22.94, 21.92, 21.11; HRMS (ESI+): m/z calcd for $C_{28}H_{36}N_3O_2$ 446.2808 [M + H]⁺; found: 446.2798.

(*S*)-*N*-(3-(3,4-dihydroisoquinolin-2(1*H*)-yl)-2-hydroxypropyl)-9-isobutyl-2,3,4,9-tetrahydro-1*H*-carbazole-6-carboxamide (**17**).

White solid; yield: 29.9%; HPLC Purity: 98.7%; ¹H NMR (300 MHz, Methanol-*d*₄) δ 8.01 (s, 1 H), 7.58 (d, *J* = 8.5 Hz, 1 H), 7.21 (d, *J* = 8.6 Hz, 1 H), 7.17–7.08 (m, 3 H), 7.08–7.00 (m, 1 H), 4.23–4.11 (m, 1 H), 3.85 (d, *J* = 7.4 Hz, 2 H), 3.77 (s, 2 H), 3.59 (d, *J* = 5.6 Hz, 1 H), 3.02–2.89 (m, 4 H), 2.79–2.60 (m, 6 H), 2.25–2.06 (m, 1 H), 2.01–1.82 (m, 4 H), 1.42–1.31 (m, 2 H), 0.93 (d, *J* = 6.5 Hz, 6 H); ¹³C NMR (75 MHz, Methanol-*d*₄) δ 170.49, 138.49, 137.13, 134.10, 133.74, 126.95, 126.25, 125.99, 125.44, 123.80, 119.29, 110.00, 108.63, 67.08, 62.47, 56.19, 51.34, 45.06, 37.51, 29.40, 28.34, 23.02, 22.86, 22.09, 20.57, 19.11, 16.79; HRMS (ESI+): m/z calcd for $C_{29}H_{38}N_3O_2$ 460.2964 [M + H]⁺; found: 460.2953.

(*S*)-9-(cyclopropylmethyl)-*N*-(3-(3,4-dihydroisoquinolin-2(1*H*)-yl)-2-hydroxypropyl)-2,3,4,9-tetrahydro-1*H*-carbazole-6-carboxamide (**18**).

White solid; yield: 48.8%; HPLC Purity: 99.8%; ¹H NMR (300 MHz, Methanol-*d*₄) δ 7.96 (d, *J* = 1.7 Hz, 1 H), 7.56–7.51 (m, 1 H), 7.20 (d, *J* = 8.6 Hz, 1 H), 7.15–7.03 (m, 3 H), 7.01–6.95 (m, 1 H), 4.17–4.06 (m, 1 H), 3.91 (d, *J* = 6.4 Hz, 2 H), 3.69 (s, 2 H), 3.61–3.46 (m, 2 H), 2.91–2.84 (m, 2 H), 2.83–2.76 (m, 2 H), 2.74–2.58 (m, 6 H), 1.97–1.89 (m, 2 H), 1.88–1.78 (m, 2 H), 1.18–1.04 (m, 1 H), 0.53–0.44 (m, 2 H), 0.36–0.24 (m, 2 H); ¹³C NMR (75 MHz, Methanol-*d*₄) δ 170.46, 138.36, 136.70, 134.18, 133.77, 128.23, 127.00, 126.22, 125.95, 125.40, 123.83, 117.13, 110.10, 108.38, 67.13, 62.50, 56.21, 51.34, 46.25, 45.05, 37.50, 28.39, 22.84, 21.95, 20.55, 11.22, 2.88; HRMS (ESI+): m/z calcd for $C_{29}H_{36}N_3O_2$ 458.2808 [M + H]⁺; found: 458.2796.

(*S*)-9-(cyclobutylmethyl)-*N*-(3-(3,4-dihydroisoquinolin-2(1*H*)-yl)-2-hydroxypropyl)-2,3,4,9-tetrahydro-1*H*-carbazole-6-carboxamide (**19**).

White solid; yield: 96.2%; HPLC Purity: 99.4%; ¹H NMR (300 MHz, Methanol-*d*₄) δ 7.95 (d, *J* = 1.8 Hz, 1 H), 7.56–7.49 (m, 1 H), 7.22 (d, *J* = 8.7 Hz, 1 H), 7.16–7.05 (m, 3 H), 7.05–6.98 (m, 1 H), 4.19–4.09 (m, 1 H), 4.04 (d, *J* = 7.0 Hz, 2 H), 3.73 (s, 2 H), 3.60–3.49 (m, 2 H), 2.92–2.83 (m, 4 H), 2.78–2.64 (m, 6 H), 2.01–1.74 (m, 10 H); ¹³C NMR (75 MHz, Methanol-*d*₄) δ 170.51, 138.50, 136.86, 134.19, 133.78, 128.23, 126.91, 126.23, 125.96, 125.41, 123.79, 119.25, 117.09, 110.00, 108.45, 67.12, 62.51, 56.23, 51.38, 45.05, 37.49, 36.61, 28.38, 25.90, 22.85, 22.05, 20.55, 17.78; HRMS (ESI+): m/z calcd for $C_{30}H_{38}N_3O_2$ 472.2964 [M + H]⁺; found: 472.2953.

(*S*)-*N*-(3-(3,4-dihydroisoquinolin-2(1*H*)-yl)-2-hydroxypropyl)-9-(oxetan-3-ylmethyl)-2,3,4,9-tetrahydro-1*H*-carbazole-6-carboxamide (**20**).

White solid; yield: 57.4%; HPLC Purity: 97.8%; ¹H NMR (400 MHz, DMSO-*d*₆) δ 7.96 (s, 1 H), 7.61–7.53 (m, 1 H), 7.33 (d, *J* = 8.6 Hz, 1 H), 7.17–7.07 (m, 3 H), 7.07–7.00 (m, 1 H), 4.74

(t, $J = 7.0$ Hz, 2 H), 4.52 (t, $J = 6.1$ Hz, 2 H), 4.42 (d, $J = 7.4$ Hz, 2 H), 4.20–4.08 (m, 1 H), 3.76 (s, 2 H), 3.60–3.53 (m, 2 H), 3.51–3.43 (m, 1 H), 2.95–2.81 (m, 4 H), 2.81–2.73 (m, 2 H), 2.73–2.61 (m, 4 H), 2.02–1.80 (m, 4 H); ^{13}C NMR (75 MHz, Methanol- d_4) δ 170.27, 138.36, 136.68, 134.21, 133.81, 128.29, 127.1) 3, 126.28, 126.02, 125.47, 124.33, 119.75, 117.33, 110.67, 108.30, 74.91, 67.16, 62.54, 56.24, 51.38, 45.12, 44.65, 35.87, 28.44, 23.01, 22.79, 22.03, 20.55; HRMS (ESI+): m/z calcd for $\text{C}_{29}\text{H}_{36}\text{N}_3\text{O}_3$ 474.2757 [M + H]⁺; found: 474.2744.

(S)-N-(3-(3,4-dihydroisoquinolin-2(1H)-yl)-2-hydroxypropyl)-2-methyl-2,3,4,5-tetrahydro-1H-pyrido[4,3-*b*]indole-8-carboxamide (**21**).

White solid; yield: 41.1%; HPLC Purity: 96.9%; ^1H NMR (300 MHz, Methanol- d_4) δ 7.98 (s, 1 H), 7.61–7.54 (m, 1 H), 7.28 (d, $J = 8.3$ Hz, 1 H), 7.20–7.10 (m, 3 H), 7.10–7.02 (m, 1 H), 4.23–4.10 (m, 1 H), 3.78 (s, 2 H), 3.73 (s, 2 H), 3.67–3.47 (m, 2 H), 3.01–2.83 (m, 8 H), 2.79–2.62 (m, 2 H), 2.59 (s, 3 H); ^{13}C NMR (75 MHz, Methanol- d_4) δ 170.44, 134.07, 133.72, 133.44, 128.27, 126.25, 126.10, 125.47, 125.38, 124.53, 119.95, 116.88, 110.23, 107.60, 67.17, 56.16, 51.34, 51.09, 45.01, 44.23, 28.31, 22.81; HRMS (ESI+): m/z calcd for $\text{C}_{25}\text{H}_{31}\text{N}_4\text{O}_2$ 419.2447 [M + H]⁺; found: 419.2449.

(S)-N-(3-(3,4-dihydroisoquinolin-2(1H)-yl)-2-hydroxypropyl)-2-ethyl-2,3,4,5-tetrahydro-1H-pyrido[4,3-*b*]indole-8-carboxamide (**22**).

White solid; yield: 30.8%; HPLC Purity: 97.0%; ^1H NMR (300 MHz, Methanol- d_4) δ 8.00 (s, 1 H), 7.61–7.54 (m, 1 H), 7.26 (d, $J = 8.5$ Hz, 1 H), 7.18–7.07 (m, 3 H), 7.06–6.94 (m, 1 H), 4.20–4.10 (m, 1 H), 3.77–3.69 (m, 4 H), 3.65–3.47 (m, 2 H), 2.96–2.80 (m, 9 H), 2.79–2.63 (m, 4 H), 1.26 (t, $J = 7.2$ Hz, 3 H); ^{13}C NMR (75 MHz, Methanol- d_4) δ 170.42, 138.55, 134.20, 133.91, 133.77, 128.23, 126.22, 126.00, 125.55, 125.42, 124.43, 119.83, 116.84, 110.20, 107.79, 67.24, 62.37, 56.19, 51.36, 49.81, 48.69, 44.97, 36.46, 28.37, 22.87, 10.97; HRMS (ESI+): m/z calcd for $\text{C}_{26}\text{H}_{33}\text{N}_4\text{O}_2$ 433.2604 [M + H]⁺; found: 433.2596.

(S)-2-cyclopropyl-N-(3-(3,4-dihydroisoquinolin-2(1H)-yl)-2-hydroxypropyl)-2,3,4,5-tetrahydro-1H-pyrido[4,3-*b*]indole-8-carboxamide (**23**).

White solid; yield: 31.9%; HPLC Purity: 98.6%; ^1H NMR (300 MHz, Methanol- d_4) δ 7.99 (d, $J = 1.7$ Hz, 1 H), 7.5–7.52 (m, 1 H), 7.23 (d, $J = 8.5$ Hz, 1 H), 7.14–7.03 (m, 3 H), 7.02–6.96 (m, 1 H), 4.18–4.07 (m, 1 H), 3.84 (s, 2 H), 3.72–3.67 (m, 2 H), 3.63–3.46 (m, 2 H), 3.04 (t, $J = 5.8$ Hz, 2 H), 2.91–2.75 (m, 8 H), 2.74–2.57 (m, 2 H), 2.02–1.92 (m, 1 H), 0.66–0.49 (m, 4 H); ^{13}C NMR (75 MHz, Methanol- d_4) δ 170.43, 138.50, 134.20, 133.85, 133.77, 128.24, 126.23, 126.01, 125.55, 125.42, 124.41, 119.81, 116.89, 110.19, 108.01, 78.98, 67.25, 62.36, 56.19, 51.33, 50.47, 49.30, 44.97, 37.74, 36.47, 28.38, 22.83, 5.02; HRMS (ESI+): m/z calcd for $\text{C}_{28}\text{H}_{35}\text{N}_4\text{O}_2$ 445.2604 [M + H]⁺; found: 445.2597.

(S)-N-(3-(3,4-dihydroisoquinolin-2(1H)-yl)-2-hydroxypropyl)-2-propyl-2,3,4,5-tetrahydro-1H-pyrido[4,3-*b*]indole-8-carboxamide (**24**).

White solid; yield: 53.3%; HPLC Purity: 99.5%; ^1H NMR (300 MHz, Methanol- d_4) δ 7.96 (d, $J = 1.7$ Hz, 1 H), 7.57–7.51 (m, 1 H), 7.25 (d, $J = 8.5$ Hz, 1 H), 4.20–4.10 (m, 1 H), 3.79–3.71 (m, 4 H), 3.61–3.46 (m, 2 H), 2.94–2.81 (m, 9 H), 2.71–2.59 (m, 2 H), 1.79–1.63 (m, 2 H), 1.01 (t, $J = 7.4$ Hz, 3 H); ^{13}C NMR (75 MHz, Methanol- d_4) δ 170.50, 138.54, 134.19, 133.89, 133.77, 128.22, 126.20, 126.00, 125.53, 125.41, 124.43, 119.79, 110.14, 107.81, 67.25, 62.35, 59.81, 56.21, 51.36, 50.31, 49.19, 44.93, 28.35, 22.84, 19.75, 10.90; HRMS (ESI+): m/z calcd for $\text{C}_{27}\text{H}_{35}\text{N}_4\text{O}_2$ 447.2760 [M + H]⁺; found: 447.2749.

(S)-N-(3-(3,4-dihydroisoquinolin-2(1H)-yl)-2-hydroxypropyl)-2-isopropyl-2,3,4,5-tetrahydro-1H-pyrido[4,3-*b*]indole-8-carboxamide (**25**).

White solid; yield: 21.2%; HPLC Purity: 96.7%; ^1H NMR (300 MHz, Methanol- d_4) δ 8.01 (d, $J = 1.7$ Hz, 1 H), 7.60–7.53 (m, 1 H), 7.26 (d, $J = 8.5$ Hz, 1 H), 7.17–7.06 (m, 3 H), 7.04–6.98 (m, 1 H), 4.20–4.10 (m, 1 H), 3.82 (s, 2 H), 3.72 (s, 2 H), 3.66–3.46 (m, 2 H), 3.08–2.98 (m, 1 H), 2.97–2.86 (m, 6 H), 2.86–2.76 (m, 2 H), 2.75–2.59 (m, 2 H), 1.22 (d, $J = 6.5$ Hz, 6 H); ^{13}C NMR (75 MHz, Methanol- d_4) δ 170.42, 138.58, 134.19, 134.04, 133.77, 128.23, 126.23, 126.00, 125.70, 125.42, 124.39, 119.81, 116.84, 110.21, 108.12, 67.26, 62.33, 56.18, 54.31, 51.33, 45.91, 44.95, 44.44, 28.36, 23.34, 17.33; HRMS (ESI+): m/z calcd for $\text{C}_{27}\text{H}_{35}\text{N}_4\text{O}_2$ 447.2760 [M + H]⁺; found: 447.2751.

(S)-N-(3-(3,4-dihydroisoquinolin-2(1H)-yl)-2-hydroxypropyl)-2-isobutyl-2,3,4,5-tetrahydro-1H-pyrido[4,3-*b*]indole-8-carboxamide (**26**).

White solid; yield: 28.0%; HPLC Purity: 99.6%; $^1\text{H-NMR}$ (300 MHz, Methanol- d_4) δ 7.97 (d, $J = 1.7$ Hz, 1 H), 7.57–7.51 (m, 1 H), 7.24 (d, $J = 8.5$ Hz, 1 H), 7.16–7.04 (m, 3 H), 7.04–6.90 (m, 1 H), 4.18–4.04 (m, 1 H), 3.70 (s, 2 H), 3.64 (s, 2 H), 3.60–3.46 (m, 2 H), 2.90–2.77 (m, 8 H), 2.72–2.59 (m, 2 H), 2.38 (d, $J = 7.2$ Hz, 2 H), 2.04–1.89 (m, 1 H), 0.98 (d, $J = 6.6$ Hz, 6 H); ^{13}C NMR (75 MHz, Methanol- d_4) δ 170.47, 138.49, 134.20, 134.13, 133.77, 128.23, 126.22, 125.99, 125.65, 125.41, 124.32, 119.71, 116.80, 110.15, 108.18, 67.25, 66.26, 56.20, 51.33, 50.68, 44.95, 36.45, 25.65, 22.89, 20.25; HRMS (ESI+): m/z calcd for $\text{C}_{28}\text{H}_{37}\text{N}_4\text{O}_2$ 461.2917 [M + H] $^+$; found: 461.2911.

3.2. Biological Activity Assay

3.2.1. PRMT5 Enzymatic Activity Inhibition Assays

The PRMT5 enzymatic activity assay was conducted by Chempartner Life science. The final concentrations of PRMT5 enzyme: 2.5 nm/L; $^3\text{H-SAM}$: 0.3 $\mu\text{M/L}$; histone peptide (H4R3S1ac): 0.3 $\mu\text{M/L}$. The protocol of radioactive methylation assay was as follows: (1) Prepare 1 \times assay buffer (modified Tris Buffer). (2) Transfer compounds to assay plate using Echo in 100% DMSO. DMSO's final fraction is 1%. (3) Prepare enzyme and $^3\text{H-SAM}$ Mix solution in 1 \times assay buffer. (4) Prepare substrate (peptide sequence ACSGRGKGGKGLGKGGAKRHRKVGK-K(Biotin)) solution in 1 \times assay buffer. (5) Transfer 15 μL of enzyme and $^3\text{H-SAM}$ solution to assay plate. (6) Incubate at room temperature for 60 min. (7) Add 10 μL of substrate solution to each well to start the reaction, and for low control transfer 10 μL of 1 \times assay buffer. (8) Incubate at room temperature for 120 min. (9) Add cold SAM in 1 \times assay buffer to make the stop mix. (10) Stop reaction with addition of 5 μL per well of stop solution. (11) Transfer 25 μL of volume per well to Flash plate from assay plate. (12) Incubate for 1 h minimum at room temperature. (13) Read plate on Micro beta. (14) Data process—get the data in Excel to obtain inhibition values using Equation (1).

$$\text{Inhibitory rate\%} = (\text{Max-Signal}) / (\text{Max-Min}) \times 100 \quad (1)$$

Fit the data in XL-Fit to obtain IC_{50} values using Equation (2):

$$Y = \text{Bottom} + (\text{Top-Bottom}) / (1 + (\text{IC}_{50}/X) \times \text{Hillslope}) \quad Y \text{ is\% inhibition and } X \text{ is compound concentration} \quad (2)$$

3.2.2. Cell Lines, Antibodies and Agents

MV-4-11 and MDA-MB-468 cell line were derived from Cell Resources Center of Shanghai Academy of life sciences (Shanghai, China). AML-12 cell line was brought from Nanjing Lixing Biotechnology Co. Ltd. (Nanjing, China). MDA-MB-468 cell line was maintained in Dulbecco's Modified Eagle Medium (DMEM, KeyGEN Bio) that contained 10% FBS (Biochannel, China), MV-4-11 cell line was maintained in Iscove's Modified Dulbecco Medium containing; 10% FBS (Biochannel, China), AML-12 cell line was maintained in DMEM/F-12 (1:1) (KeyGEN, China; 1% ITS Liquid Media Supplement (Sigma, America), dexamethasone 40 ng/mL (Sigma, USA) and 10% FBS (Biochannel, China). All cells were grown in a humidified incubator containing 5% carbon dioxide at 37 $^{\circ}\text{C}$. All compounds were dispersed in dimethyl sulfoxide (Sigma), the concentration of the reserve solution was 10 mmol/L and the solution was stored in a refrigerator at -20 $^{\circ}\text{C}$. SDMA (# 13222S), β -Tubulin (#2146S) and horseradish peroxidase (HRP)-linked secondary antibodies anti-rabbit or anti-mouse IgG were purchased from Cell Signaling Technology (CST), and the anti-PRMT5 (ab109451) antibody was purchased from ABCAM.

3.2.3. Anti-Proliferation Cells Assay of Compounds

The antiproliferative activities of compounds in vitro were measured by CellTiter-Glo (CTG) assay (Promega, America). In linear/log-phase growth, cultured MV-4-11 cells were split to with seeding density of 2×10^5 cells/mL in 1–20 mL of media, depending on the yield required at the end of the growth period. At the conclusion of each treatment period, cells were harvested by centrifugation (4 min, 1000 rpm), and cell pellets were

rinsed twice with PBS before being research further processing. Afterwards, cells were plated in 96-well plates with a density of 500 cells/well in 1 mL media. After six hours incubation, compounds treatment was performed. Half of the culture medium was moved and re-plated with fresh media with fresh compound after 6 days. On the 12th day, Cell Titer-Glo Luminescent Cell Viability assays (Promega, USA) were used to determine the viable cell number, and luminescence was recorded using the Envision Multilabel Plate Readers (PerkinElmer). The concentration dependence curves were determined at each time point using GraphPad Prism 8.0 software.

3.2.4. Western Blot Assays

Compounds were administered at the expected concentration for the expected time in MV-4-11 cell lines. After being washed twice with PBS, cells were lysed with RIPA buffer, protease inhibitors (PMSF, MCE, New York, NY, USA), and phosphatase cocktails II (MCE, USA) for 1 h. The mixture was centrifuged at 12000 rpm for 15 min. The total protein content was quantified by BCA kit (Beyotime, Shanghai, China). Equivalent proteins were electrophoresed through 8~10% SDS-PAGE and then transferred on to polyvinylidene difluoride membranes (Millipore, Burlington, MA, USA). Subsequently, block the membrane for 1~2 h by 5% (*w/v*) skim milk (BD, Columbus, OH, USA). Proteins were detected using primary antibodies, followed by HRP-conjugated secondary antibodies, and visualization was performed using ECL (Vazyme Biotech, Beijing, China) as the HRP substrate. The target blots were detected with chemiluminescence system (Tanon, Shanghai, China). The densitometric analysis was performed with Image J software.

Tumor tissue was grinded by a cryo-grinder before being lysed with an RIPA buffer, protease inhibitors (PMSF, MCE), and phosphatase cocktails II (MCE). The mixture was centrifuged for 15 min (12,000 rpm). The following steps were the same as with cells.

3.2.5. CETSAs

The cellular thermal shift assay and the isothermal dose response were run as previously described. Briefly, MV-4-11 cells were collected and centrifuged (4 min, 1000 rpm) and washed twice with PBS. Then the cells were divided three equal parts with seeding density of 1×10^6 cells/mL into 60 mm cell culture dish in three mL media. The cell suspension was incubated with DMSO and compounds for 18 h at 37 °C, 5% CO₂, and 85% RH.

After incubation, cells were collected and washed twice with PBS. Then they divided the ten parts into transferred thin-walled PCR tubes (0.2 mL, Axygen, Union City, CA, USA) in 50 µL PBS. Cells were subjected to 3 min of heat in 96-well thermal cycler (Eppendorf Mastercycler nexus GSX1, Düsseldorf, German) at temperatures of 37, 46, 49, 52, 55, 58, 61, 64, 67 and 70 °C. After heating, cells were left to cool for 3 min and then snap frozen in −80 °C ultra-low temperature freezer overnight. The next day, cells were subjected to 3 rapid freeze thaws with 15 s of vortexing after each thaw. Cell lysates were centrifuged at 12000 rpm for 10 min to separate the soluble fractions from precipitates, and the supernatant was transferred (~40 µL) to 1.5 mL Eppendorf tube and 8 µL 6 × Loading Buffer, stored at −80 °C until analysis. Western blot step was the same as cells and tumor tissue.

3.2.6. Pharmacokinetic Study in Mice

The pharmacokinetic properties were evaluated by PRECEDO. China. SPF ICR mice (18–20 g, 6–8 weeks, *n* = 3 per group) were used to carried out pharmacokinetics determinations. The compound was formulated into 0.4 mg/mL test solution with DMSO, PEG400 and 5% glucose injection and administered intravenously at a dose of 1 mg/kg. Collecting samples at different times after treatment. Plasma was obtained from the blood samples by centrifugation (6000 rpm for 3 min at 2–8 °C) and stored at −20 °C. The LC-MS/MS (Shimadzu, API 4000) method was used to determine the concentration of each animal at each time point.

3.2.7. In Vivo Xenograft Research

Male BALB/c nude mice (6–8 weeks old) were purchased from Hangzhou Medical College. All animals were housed in a specific pathogen-free facility. MV-4-11 cells (5×10^6) suspended in 0.2 mL of PBS were inoculated subcutaneously on the right flank of each BALB/c nude mouse. Mice were divided randomly (5 mice for each group) into two treatment groups and a control group when the size of the tumors reached 150 mm³. GSK-3326595 (10 mg/kg, dissolved in DMSO/10% PEG300/20% β -cyclodextrin/7%), compound 20 (10 mg/kg, DMSO/10% PEG300/20% β -cyclodextrin/7%) and vehicle (DMSO/10% PEG300/20% β -cyclodextrin/7%) were administered twice per day for 28 days by intraperitoneal administration. The tumor volume and body weight were measured every 2 days. The tumor volume was determined with Vernier calipers and calculated as follows: tumor volume = $a \times b^2/2$, where a and b stand for the longest and shortest diameters measured by the vernier caliper, respectively. All animal experiments have been approved by Pharmaceutical Experiment Center of China Pharmaceutical University.

3.2.8. H&E Staining

The tumor tissue samples of xenograft model mice were fixed with 4% paraformaldehyde, dehydrated with ethanol, immersed in xylene, embedded in paraffin and cut into 4.0 μ m longitudinal sections. The paraffin-embedded sections were stained with H&E according to the manufacturer's instructions (Beyotime, Shanghai, China). Each group of samples was observed with a DM6B-positive fluorescence microscope (Leica, Frankfurt, Germany). Five images were randomly captured per slide.

3.2.9. Immunohistochemical Staining

Tumors of xenograft model mice were embedded in paraffin, incubated with 0.3% hydrogen peroxide to block endogenous peroxidase, blocked with 1.0% BSA, stained with the primary antibody, incubated with secondary antibody and counterstained with hematoxylin. Each group was examined using the DM6B-positive fluorescence microscope (Leica, Germany). Five images were randomly captured per slide. The percentage of stained dots were analyzed by Image J software.

3.2.10. Statistical Analysis

Data were analyzed using Prism 8.0. Results were expressed as means \pm SD. Differences between treatment regimens were analyzed by one way ANOVA. $p < 0.05$ was considered statistical significance.

3.3. Molecular Modelling

The protein crystallized was downloaded from the PDB (PDB code: 4X61). Protein Preparation Wizard of the Schrodinger Suite was used to prepare protein structure to ensure that the downloaded X-ray structure was reliable and qualitatively considerable for further in silico studies. Small molecules were prepared using LigPrep [30] prior to docking simulation to obtain the accessible least-energy ionized conformer and tautomeric states of the ligands. The binding site was defined by a box centered on the centroid of the crystal ligand and with similar size to the ligand. The Glide implemented in Schrodinger 2009 was used for molecular docking [31]. The standard precision (SP) mode was used for the docking and scoring. All other parameters were kept default. The best pose was output on the basis of Glide score and the protein–ligand interactions. PyMOL software was employed to depict structural representations [32].

4. Conclusions

In this work, we designed and synthesized a series of THIQ derivatives. Among them, compound 20 has potent PRMT5 inhibitory activity, with the IC₅₀ value of 4.2 nM. In addition, compound 20 also dramatically suppresses the growth of MV-4-11 and MDA-MB-468 cell lines with no significant cytotoxicity in normal hepatocyte AML-12 cell lines. In

MV-4-11 cell-derived xenograft model, compound **20** (TGI = 47.6%) at a dose of 10 mg/kg (iv) displays more effective antitumor effects than **GSK-3326595** (TGI = 39.3%) at the same dose (iv). The preliminary mechanism studies in vivo confirm that **20** exerts antitumor effect via decreasing the expression of sDMA in tumor tissues. Encouraging to researchers owing to the excellent properties in vitro and in vivo, **20** as a novel PRMT5 inhibitor is worthy of further study.

Supplementary Materials: The following supporting information can be downloaded at: <https://www.mdpi.com/article/10.3390/molecules27196637/s1>. Figure S1: Plasma concentration curve after administration of **20** (2 mg/kg, iv). The value at each time point represents. Figure S2: Plasma concentration curve after administration of **20** (10 mg/kg, ig). The value at each time point represents. Table S1: intravenous injection of 2 mg/kg compound **20** in male mice pharmacokinetic parameters. Table S2: gavage of 10 mg/kg compound **20** in male mice pharmacokinetic parameters.

Author Contributions: Designed and synthesized the target compounds, Y.T., X.C. and J.H.; in vitro anti-proliferation assay, S.H., S.W. and Q.L.; In vivo antitumor activity evaluation, S.H., Y.T. and L.H.; software, Y.Z.; writing—original draft preparation, Y.T. and S.H.; writing—review and editing, Q.Z., Y.Z. and Y.X.; funding acquisition, Q.Z. and Y.X. All authors have read and agreed to the published version of the manuscript.

Funding: This research was funded by the Fundamental Research Funds for the Central Universities (2632021ZD14).

Institutional Review Board Statement: Not applicable.

Informed Consent Statement: Not applicable.

Data Availability Statement: The article contains complete data used to support the findings of this study.

Acknowledgments: Thank you for support of the public platform of the State Key Laboratory of Natural Medicines, China Pharmaceutical University.

Conflicts of Interest: The authors declare that they have no known competing financial interests or personal relationships that could have appeared to influence the work reported in this paper.

Sample Availability: Samples of the compounds described in this paper are available from the authors.

References

1. Jarrold, J.; Davies, C.C. PRMTs and arginine methylation: Cancer's best-kept secret? *Trends Mol. Med.* **2019**, *25*, 993–1009. [[CrossRef](#)]
2. Yang, Y.; Hadjikyriacou, A.; Xia, Z.; Gayatri, S.; Kim, D.; Zurita-Lopez, C.; Kelly, R.; Guo, A.; Li, W.; Clarke, S.G. PRMT9 is a type II methyltransferase that methylates the splicing factor SAP145. *Nat. Commun.* **2015**, *6*, 6428. [[CrossRef](#)]
3. Yang, Y.; Bedford, M.T. Protein arginine methyltransferases and cancer. *Nat. Rev. Cancer* **2013**, *13*, 37–50. [[CrossRef](#)] [[PubMed](#)]
4. Feng, Y.; Maity, R.; Whitelegge, J.P.; Hadjikyriacou, A.; Li, Z.; Zurita-Lopez, C.; Al-Hadid, Q.; Clark, A.T.; Bedford, M.T.; Masson, J.-Y. Mammalian protein arginine methyltransferase 7 (PRMT7) specifically targets RXR sites in lysine- and arginine-rich regions. *J. Biol. Chem.* **2013**, *288*, 37010–37025. [[CrossRef](#)]
5. Auclair, Y.; Richard, S. The role of arginine methylation in the DNA damage response. *DNA Repair* **2013**, *12*, 459–465. [[CrossRef](#)]
6. Pollack, B.P.; Kotenko, S.V.; He, W.; Izotova, L.S.; Barnoski, B.L.; Pestka, S. The human homologue of the yeast proteins Skb1 and Hsl7p interacts with Jak kinases and contains protein methyltransferase activity. *J. Biol. Chem.* **1999**, *274*, 31531–31542. [[CrossRef](#)]
7. Antonysamy, S.; Bonday, Z.; Campbell, R.M.; Doyle, B.; Druzina, Z.; Gheyi, T.; Han, B.; Jungheim, L.N.; Qian, Y.; Rauch, C. Crystal structure of the human PRMT5: MEP50 complex. *Proc. Natl. Acad. Sci. USA* **2012**, *109*, 17960–17965. [[CrossRef](#)]
8. Tae, S.; Karkhanis, V.; Velasco, K.; Yaneva, M.; Erdjument-Bromage, H.; Tempst, P.; Sif, S. Bromodomain protein 7 interacts with PRMT5 and PRC2, and is involved in transcriptional repression of their target genes. *Nucleic Acids Res.* **2011**, *39*, 5424–5438. [[CrossRef](#)]
9. Pal, S.; Vishwanath, S.N.; Erdjument-Bromage, H.; Tempst, P.; Sif, S. Human SWI/SNF-associated PRMT5 methylates histone H3 arginine 8 and negatively regulates expression of ST7 and NM23 tumor suppressor genes. *Mol. Cell. Biol.* **2004**, *24*, 9630–9645. [[CrossRef](#)]
10. Xiao, W.; Chen, X.; Liu, L.; Shu, Y.; Zhang, M.; Zhong, Y. Role of protein arginine methyltransferase 5 in human cancers. *Biomed. Pharmacother.* **2019**, *114*, 108790. [[CrossRef](#)]
11. Zhu, F.; Rui, L. PRMT5 in gene regulation and hematologic malignancies. *Genes Dis.* **2019**, *6*, 247–257. [[CrossRef](#)]

12. Lin, H.; Luengo, J.I. Nucleoside protein arginine methyltransferase 5 (PRMT5) inhibitors. *Bioorg. Med. Chem. Lett.* **2019**, *29*, 1264–1269. [[CrossRef](#)]
13. Shailesh, H.; Zakaria, Z.Z.; Baiocchi, R.; Sif, S. Protein arginine methyltransferase 5 (PRMT5) dysregulation in cancer. *Oncotarget* **2018**, *9*, 36705. [[CrossRef](#)]
14. Wang, Y.; Hu, W.; Yuan, Y. Protein arginine methyltransferase 5 (PRMT5) as an anticancer target and its inhibitor discovery. *J. Med. Chem.* **2018**, *61*, 9429–9441. [[CrossRef](#)]
15. Prabhu, L.; Wei, H.; Chen, L.; Demir, Ö.; Sandusky, G.; Sun, E.; Wang, J.; Mo, J.; Zeng, L.; Fishel, M. Adapting AlphaLISA high throughput screen to discover a novel small-molecule inhibitor targeting protein arginine methyltransferase 5 in pancreatic and colorectal cancers. *Oncotarget* **2017**, *8*, 39963. [[CrossRef](#)]
16. Kim, H.; Kim, H.; Feng, Y.; Li, Y.; Tamiya, H.; Tocci, S.; Ronai, Z.E.A. PRMT5 control of cGAS/STING and NLRC5 pathways defines melanoma response to antitumor immunity. *Sci. Transl. Med.* **2020**, *12*, eaaz5683. [[CrossRef](#)]
17. Luo, Y.; Gao, Y.; Liu, W.; Yang, Y.; Jiang, J.; Wang, Y.; Tang, W.; Yang, S.; Sun, L.; Cai, J. MYC-Protein Arginine Methyltransferase 5 Axis Defines the Tumorigenesis and Immune Response in Hepatocellular Carcinoma. *Hepatology* **2021**, *74*, 1932–1951. [[CrossRef](#)]
18. Ma, D.; Yang, M.; Wang, Q.; Sun, C.; Shi, H.; Jing, W.; Bi, Y.; Shen, X.; Ma, X.; Qin, Z. Arginine methyltransferase PRMT5 negatively regulates cGAS-mediated antiviral immune response. *Sci. Adv.* **2021**, *7*, eabc1834. [[CrossRef](#)]
19. Duncan, K.W.; Chesworth, R.; Boriack-Sjodin, P.A.; Munchhof, M.J.; Jin, L. PRMT5 Inhibitors and Uses Thereof. US8940726B2, December 2014. Available online: <https://www.freepatentsonline.com/US8940726B2.html> (accessed on 4 August 2014).
20. Chan-Penebre, E.; Kuplast, K.; Majer, C.; Boriack-Sjodin, P.; Wigle, T.; Johnston, L. A Selective Inhibitor of PRMT5 with In Vivo and In Vitro Potency in MCL Models. *Nat. Chem. Biol.* **2015**, *11*, 432–437. [[CrossRef](#)]
21. Brehmer, D.; Beke, L.; Wu, T.; Millar, H.J.; Moy, C.; Sun, W.; Mannens, G.; Pande, V.; Boeckx, A.; van Heerde, E. Discovery and pharmacological characterization of JNJ-64619178, a novel small-molecule inhibitor of PRMT5 with potent antitumor activity. *Mol. Cancer Ther.* **2021**, *20*, 2317–2328. [[CrossRef](#)] [[PubMed](#)]
22. Ohno, H.; Kubo, K.; Murooka, H.; Kobayashi, Y.; Nishitoba, T.; Shibuya, M.; Yoneda, T.; Isoe, T. A c-fms tyrosine kinase inhibitor, Ki20227, suppresses osteoclast differentiation and osteolytic bone destruction in a bone metastasis model. *Mol. Cancer Ther.* **2006**, *5*, 2634–2643. [[CrossRef](#)] [[PubMed](#)]
23. Palte, R.L.; Schneider, S.E.; Altman, M.D.; Hayes, R.P.; Kawamura, S.; Lacey, B.M.; Mansueto, M.S.; Reutershan, M.; Siliphaivanh, P.; Sondey, C. Allosteric modulation of protein arginine methyltransferase 5 (PRMT5). *ACS Med. Chem. Lett.* **2020**, *11*, 1688–1693. [[CrossRef](#)] [[PubMed](#)]
24. Lin, H.; Wang, M.; Zhang, Y.W.; Tong, S.; Leal, R.A.; Shetty, R.; Vaddi, K.; Luengo, J.I. Discovery of potent and selective covalent protein arginine methyltransferase 5 (PRMT5) inhibitors. *ACS Med. Chem. Lett.* **2019**, *10*, 1033–1038. [[CrossRef](#)]
25. Shen, Y.; Gao, G.; Yu, X.; Kim, H.; Wang, L.; Xie, L.; Schwarz, M.; Chen, X.; Guccione, E.; Liu, J. Discovery of first-in-class protein arginine methyltransferase 5 (PRMT5) degraders. *J. Med. Chem.* **2020**, *63*, 9977–9989. [[CrossRef](#)] [[PubMed](#)]
26. Jafari, R.; Almqvist, H.; Axelsson, H.; Ignatushchenko, M.; Lundbäck, T.; Nordlund, P.; Molina, D.M. The cellular thermal shift assay for evaluating drug target interactions in cells. *Nat. Protoc.* **2014**, *9*, 2100–2122. [[CrossRef](#)] [[PubMed](#)]
27. Zachos, J.C.; Rohl, U.; Schellenberg, S.A.; Sluijs, A.; Hodell, D.A.; Kelly, D.C.; Thomas, E.; Nicolo, M.; Raffi, I.; Lourens, L.J. Rapid acidification of the ocean during the Paleocene-Eocene thermal maximum. *Science* **2005**, *308*, 1611–1615. [[CrossRef](#)] [[PubMed](#)]
28. Afridi, H.I.; Kazi, T.G.; Talpur, F.N.; Naher, S.; Brabazon, D. Relationship between toxic metals exposure via cigarette smoking and rheumatoid arthritis. *Clin. Lab.* **2014**, *60*, 1735–1745. [[CrossRef](#)] [[PubMed](#)]
29. Humphrey, P.A. Histopathology of prostate cancer. *Cold Spring Harb. Perspect. Med.* **2017**, *7*, a030411. [[CrossRef](#)] [[PubMed](#)]
30. *LigPrep*; Version 2.3.; Schrödinger, LLC.: New York, NY, USA, 2009.
31. *Glide*; Version 5.5.; Schrödinger, LLC.: New York, NY, USA, 2009.
32. *The PyMOL Molecular Graphics System*; Version 2.6.0a0.; Schrödinger, LLC.: New York, NY, USA, 2009.